Retinal Dystrophies Associated With Peripherin-2: Genetic Spectrum and Novel Clinical Observations in 241 Patients

Rachael C. Heath Jeffery,[1–3] Jennifer A. Thompson,[4] Johnny Lo,[5] Enid S. Chelva,[4] Sean Armstrong,[1,4] Jose S. Pulido,[6] Rebecca Procopio,[6] Andrea L. Vincent,[7,8] Lorenzo Bianco,[9] Maurizio Battaglia Parodi,[9] Lucia Ziccardi,[10] Giulio Antonelli,[10] Lucilla Barbano,[10] João P. Marques,[11] Sara Geada,[11] Ana L. Carvalho,[12] Wei C. Tang,[13,14] Choi M. Chan,[13,14] Camiel J. F. Boon,[15,16] Jonathan Hensman,[16] Ta-Ching Chen,[17,18] Chien-Yu Lin,[17] Pei-Lung Chen,[17] Ajoy Vincent,[19] Anupreet Tumber,[19] Elise Heon,[19] John R. Grigg,[20,21] Robyn V. Jamieson,[20,21] Elisa E. Cornish,[20] Benjamin M. Nash,[21,22] Shyamanga Borooah,[23,24] Lauren N. Ayton,[25–27] Alexis Ceecee Britten-Jones,[25–27] Thomas L. Edwards,[25–27] Jonathan B. Ruddle,[25,26] Abhishek Sharma,[28] Rowan G. Porter,[29] Tina M. Lamey,[4] Terri L. McLaren,[1,4] Samuel McLenachan,[1] Danial Roshandel,[1] and Fred K. Chen[1–4,26,27]

[1]Centre for Ophthalmology and Visual Science, The University of Western Australia, Perth, Western Australia, Australia
[2]Ocular Tissue Engineering Laboratory, Lions Eye Institute, Nedlands, Western Australia, Australia
[3]Royal Victorian Eye and Ear Hospital, East Melbourne, Victoria, Australia
[4]Australian Inherited Retinal Disease Registry and DNA Bank, Department of Medical Technology and Physics, Sir Charles Gairdner Hospital, Nedlands, Western Australia, Australia
[5]School of Science, Edith Cowan University, Perth, Western Australia, Australia
[6]Wills Eye Hospital, Mid Atlantic Retina, Thomas Jefferson University, Philadelphia, PA, United States
[7]Department of Ophthalmology, FMHS, New Zealand National Eye Centre, University of Auckland, Auckland, New Zealand
[8]Eye Department, Greenlane Clinical Centre, Auckland District Health Board, Auckland, New Zealand
[9]Department of Ophthalmology, IRCCS San Raffaele Scientific Institute, Milan, Italy
[10]IRCCS-Fondazione Bietti, Rome, Italy
[11]Ophthalmology Unit, Centro Hospitalar e Universitário de Coimbra (CHUC), Clinical and Academic Centre of Coimbra (CACC), Coimbra, Portugal
[12]Medical Genetics Unit, Centro Hospitalar e Universitário de Coimbra (CHUC), Coimbra, Portugal
[13]Singapore National Eye Centre, Singapore, Singapore
[14]Singapore Eye Research Institute, Singapore, Singapore
[15]Department of Ophthalmology, Leiden University Medical Center, Leiden, the Netherlands
[16]Department of Ophthalmology, Amsterdam University Medical Center, University of Amsterdam, the Netherlands
[17]Department of Ophthalmology, National Taiwan University Hospital, Taipei, Taiwan
[18]Center of Frontier Medicine, National Taiwan University Hospital, Taipei, Taiwan
[19]Department of Ophthalmology, Hospital for Sick Children, Toronto, Ontario, Canada
[20]Save Sight Institute, Faculty of Medicine and Health, The University of Sydney, Sydney, Australia
[21]Eye Genetics Research Unit, Children's Medical Research Institute, The Children's Hospital at Westmead, Sydney, New South Wales, Australia
[22]Sydney Genome Diagnostics, Western Sydney Genetics Program, Sydney Children's Hospitals Network, Sydney, New South Wales, Australia
[23]University of California San Diego, La Jolla, California
[24]The Viterbi Family Department of Ophthalmology and Shiley Eye Institute, University of California San Diego, La Jolla, CA, United States
[25]Department of Optometry and Vision Sciences, University of Melbourne, Melbourne, Victoria, Australia
[26]Centre for Eye Research Australia, Royal Victorian Eye and Ear Hospital, Melbourne, Victoria, Australia
[27]Ophthalmology, Department of Surgery, University of Melbourne, Melbourne, Victoria, Australia
[28]Ophthalmology Department, Royal Brisbane and Women's Hospital, Brisbane, Australia
[29]Southern Queensland Centre of Excellence, Inala, Australia

Correspondence: Fred K. Chen, Lions Eye Institute, 2 Verdun Street, Nedlands, WA 6009, Australia; fred.chen@lei.org.au.

Purpose. To describe the clinical, electrophysiological and genetic spectrum of inherited retinal diseases associated with variants in the PRPH2 gene.

Methods. A total of 241 patients from 168 families across 15 sites in 9 countries with pathogenic or likely pathogenic variants in PRPH2 were included. Records were reviewed for age at symptom onset, visual acuity, full-field ERG, fundus colour photography, fundus

Investigative Ophthalmology & Visual Science

iovs.arvojournals.org | ISSN: 1552-5783

Received: February 10, 2024
Accepted: April 12, 2024
Published: May 14, 2024

Citation: Heath Jeffery RC, Thompson JA, Lo J, et al. Retinal dystrophies associated with peripherin-2: genetic spectrum and novel clinical observations in 241 patients. *Invest Ophthalmol Vis Sci*. 2024;65(5):22. https://doi.org/10.1167/iovs.65.5.22

autofluorescence (FAF), and SD-OCT. Images were graded into six phenotypes. Statistical analyses were performed to determine genotype–phenotype correlations.

Results. The median age at symptom onset was 40 years (range, 4–78 years). FAF phenotypes included normal (5%), butterfly pattern dystrophy, or vitelliform macular dystrophy (11%), central areolar choroidal dystrophy (28%), pseudo-Stargardt pattern dystrophy (41%), and retinitis pigmentosa (25%). Symptom onset was earlier in retinitis pigmentosa as compared with pseudo-Stargardt pattern dystrophy (34 vs 44 years; $P = 0.004$). The median visual acuity was 0.18 logMAR (interquartile range, 0–0.54 logMAR) and 0.18 logMAR (interquartile range 0–0.42 logMAR) in the right and left eyes, respectively. ERG showed a significantly reduced amplitude across all components ($P < 0.001$) and a peak time delay in the light-adapted 30-Hz flicker and single-flash b-wave ($P < 0.001$). Twenty-two variants were novel. The central areolar choroidal dystrophy phenotype was associated with 13 missense variants. The remaining variants showed marked phenotypic variability.

Conclusions. We described six distinct FAF phenotypes associated with variants in the PRPH2 gene. One FAF phenotype may have multiple ERG phenotypes, demonstrating a discordance between structure and function. Given the vast spectrum of PRPH2 disease our findings are useful for future clinical trials.

Keywords: pattern dystrophy, peripherinopathy, OCT, fundus autofluorescence, CACD

Inherited retinal diseases (IRDs) are the most common cause of blindness in the working age group.[1] Disease-associated variants in the *PRPH2* gene were the fourth most common cause of IRD (5.2%) in the United Kingdom.[2] To date, 352 disease-causing variants in *PRPH2* are listed in the Human Gene Mutation Database with autosomal dominant, and less commonly, recessive and digenic (with *retinal outer segment membrane protein 1*, *ROM1,* OMIM*180721) inheritance.[3] *PRPH2* (OMIM *179605), encodes a photoreceptor-specific tetraspanin, essential for the formation and maintenance of rod and cone outer segments.[4] Dominant variants in *PRPH2* lead to central areolar choroidal dystrophy (CACD, OMIM #613105), retinitis pigmentosa (RP7, OMIM #608133), pseudo-Stargardt pattern dystrophy (PSPD, OMIM #169150), butterfly pattern dystrophy (BPD), and vitelliform macular dystrophy (VMD, OMIM #608161). Disease-associated variants in the *PRPH2* gene have been reported in pedigrees with marked interfamilial and intrafamilial variability and penetrance.[4,5]

To date, no clear genotype–phenotype correlations in human *PRPH2* disease have been firmly established.[4,6–9] This may be attributable to the relatively small sample sizes of previous clinical studies, variable penetrance, and no standardized system for phenotype grading using multimodal imaging. Some variability may be due to genetic modifiers in *ROM1* and *ABCA4*.[7,8] Poloschek et al.[7] found patients who carry the p.Arg172Trp variant in *PRPH2* demonstrated an isolated MD, whereas those carrying additional variants in the *ROM1* or *ABCA4* gene exhibited a more severe phenotype. However, Leroy et al.[8] excluded variants in *ROM1* as a modifier for an RP phenotype in *PRPH2* disease. A recent case series of 19 *PRPH2* patients by Bianco et al.[9] proposed that missense variants in the D2 loop were associated with a cone–rod dystrophy (CRD). To date, pathogenic missense variants at six codon positions (Arg142, Arg172, Arg195, Ile196, Arg203, and Gly208) have been reported to cause CACD.[9–17] In contrast, truncating variants (nonsense and frameshift) have been associated with a range of phenotypes including VMD, BPD, PSPD, and RP.

This study describes the clinical and genetic spectrum of *PRPH2*-associated IRD, including 22 novel pathogenic variants. Herein we report genotype–phenotype correlations in the largest multicenter case series of 241 patients harbouring 91 unique pathogenic or likely pathogenic *PRPH2* variants. Given the marked variability of disease, our findings will be useful for defining cohorts for inclusion in future clinical trials.

Methods

Study Population

A retrospective cohort study of patients carrying a pathogenic or likely pathogenic variant in the *PRPH2* gene. Family members carrying the same variant were also included where available. Patients were identified from the Australian Inherited Retinal Diseases Registry and DNA bank with phenotypic data acquired through the Western Australia Retinal Degeneration Study, an extensive database for IRDs that currently includes more than 900 patients referred from 2017 to December 2023 at the Lions Eye Institute (Perth, Australia). Additional data were collected from the Centre for Eye Research Australia (Melbourne, Australia), Save Sight Institute (Sydney, Australia), Royal Brisbane and Women's Hospital (Brisbane, Australia), New Zealand National Eye Centre (Auckland, New Zealand), IRCCS Fondazione Bietti (Rome, Italy), IRCCS San Raffaele Scientific Institute (Milan, Italy), IRD-PT registry[18] (Coimbra, Portugal), Amsterdam University Medical Centers (Amsterdam, the Netherlands), National Taiwan University Hospital, (Taipei, Taiwan), Singapore National Eye Centre (Singapore, Singapore), The Hospital for Sick Children (Toronto, Ontario, Canada), Shiley Eye Institute, University of California San Diego (San Diego, CA, USA), and Wills Eye Hospital (Philadelphia, PA, USA).

This study was approved by the institutional review boards of the University of Western Australia (2021/ET000151), Sir Charles Gairdner Hospital (RGS04985, 1998-115), Royal Victorian Eye and Ear Hospital/Centre for Eye Research Australia (19/1443H), New Zealand Ministry of Health (NTX/08/12/123), Auckland District Health Board (A+4290), the Save Sight Institute (2022/PID01932), Sezione IFO/Fondazione Bietti (NEU_01-2014), Vita-Salute San Raffaele University (MIRD2020), University of Coimbra (CE-125/2019), Erasmus Medical Center (NL34152.078.10),

National Taiwan University Hospital (IRB 201408082RINC), Singapore ethics review board (2015/2766), University of California San Diego (IRB 120516), Wills Eye Hospital (IRB 2021-85), and the Hospital for Sick Children (REB-1000017804). It adhered to the tenets of the Declaration of Helsinki, and informed consent was obtained from all participants or their legal guardians.

Clinical Data Collection

Data were collected for age at symptom onset, family history, visual acuity (VA), electrophysiological testing, and clinical imaging, including SD-OCT, fundus autofluorescence (FAF), and colour imaging. Age at onset was defined as the year in which the first symptoms were noted. VA was measured on either a Snellen-style or a logMAR-style chart, such as the Early Treatment Diabetic Retinopathy letter chart. Optos ultrawide field FAF imaging (Optos PLC, Dunfermline, UK) was used for phenotype grading where possible. Heidelberg HRA+OCT (Heidelberg Engineering, Heidelberg, Germany) 55° or 30° blue wavelength FAF images were graded when Optos images were not available. All SD-OCT scans were obtained using Heidelberg Spectralis.

FAF grading was performed by two independent examiners (FKC and RCHJ) and included the following phenotypes: normal, VMD, BPD, CACD, PSPD, and RP. The CACD phenotype, as originally described by Hoyng et al.[19] and Boon et al.,[20] had a well-defined oval region of stippled hyper and hypoautofluorescence in the central macular with or without a radial configuration of hyperautfluorescence at the border and hypoautofluorescent patches within.[19] As per Boon et al.[20] using color, FAF, and fluorescein angiography, CACD may reach the temporal vascular arcade superiorly and inferiorly and encompass the optic nerve, nasally with no peripapillary sparing. We only included cases with stages 2 to 4 of the Hoyng et al.[19] classification system, which was based on color and fluorescein angiography. This was due to the difficulty in distinguishing stage 1 CACD from VMD or BPD. The PSPD phenotype included focal hyperautofluorscent or fleck-like lesions, with or without stippled hypoautofluorescence spreading, centrifugally beyond the arcades resembling Stargardt disease. The RP phenotype was characterized by peripheral hypoautofluorescence with or without a central hyperautofluorscent ring. Any grading disagreements were resolved by a third examiner (CJFB).

Electrophysiology was performed in accordance with the International Clinical Electrophysiology of Vision Society Standards.[21–23] Full-field ERG traces were reviewed, and component parameters were extracted and compared with a control cohort at Sir Charles Gairdner Hospital, Perth, Australia. A cone dystrophy (COD) was noted if the light-adapted (LA) responses showed a-wave reduction and flicker delay, whereas the dark-adapted (DA) responses were within the normal range. CRD was defined by a more severe LA than DA response component deficit. A rod–cone dystrophy (RCD) was defined by a more severe DA than LA response component deficit (typically with no signal detectable in the DA 0.01 cd/m^2 test). MD was defined by a reduced P50 on the pattern ERG (PERG) or central response density loss on multifocal ERG with the DA and LA response components within the normal range.

Some of these cases have been published previously by Heath Jeffery et al.[24] (n = 12), Bianco et al.[9] (n = 19), and Antonelli et al.[25] (n = 28).

Genetic Data Collection

Variants in the *PRPH2* gene were identified using a range of molecular strategies over time. All variants were confirmed with Sanger sequencing or whole exome sequencing. Genetic testing was performed with next-generation sequencing. Pathogenicity of *PRPH2* variants was assigned based on the American College of Medical Genetics and Genomics guidelines and associated literature.[26,27] Previous disease associations were explored in the Human Gene Mutation Database, Leiden Open Variation Database (http://databases.lovd.nl/shared/genes/PRPH2), and ClinVar (https://www.ncbi.nlm.nih.gov/clinvar/). Potential pathogenicity of variants was assessed in silico with different tools, including functional pathogenicity and protein stability predictors using PolyPhen2,[28] SIFT,[29] REVEL,[30] and CADD[31] for missense variants, SIFT-Indel[32,33] and VEST-4[34] for in-frame amino acid alterations and frameshift variants, Mutation Taster[35] and ENTPRISE-X[36] for nonsense and delins, and Splice AI[37] for splicing-altering variants.

Statistical Analyses

All analyses were performed in R software version 4.1.3 (The R Core Team, Vienna, Austria) and R Studio version 2022.07.1 (RStudio Team, Boston, MA, USA). Categorical data was expressed as proportions, and continuous data as means with standard deviations or a median and interquartile range (IQR). For genotype–phenotype correlations, genotypes were stratified into exon deletions, missense, in-frame indels, frameshift, nonsense, splicing, and start–loss. Clinical features considered for statistical analysis were age at symptom onset, VA, FAF grading, and ERG parameters. Visual impairment was recorded according to the World Health Organization: mild (VA, <20/40 and ≥20/60), moderate (VA, <20/60 and ≥20/200), severe (VA, <20/200 and ≥20/400), and blindness (VA, <20/400). VA data measured on a Snellen-style chart was converted to logMAR equivalent, and off-chart levels of vision were assigned a logMAR value of 2.0 for counting fingers, 2.3 for hand movements, and 2.6 for light perception. A locally estimated scatterplot smoothing curve was constructed using VA from the better-seeing eye (lowest logMAR value) to illustrate the average evolution of VA with age across the cohort. Interocular symmetry in VA was determined by Bland-Altman analysis and Spearman rho. One-way ANOVA and Kruskal–Wallis testing compared clinical variables across different FAF phenotypes. Mann–Whitney U testing was used to compare ERG parameters in the *PRPH2* cohort with controls. Bonferroni correction was applied, where appropriate, for post hoc comparisons and multiple testing. Statistical significance was set at a P value of less than 0.05.

Results

Clinical Presentation and Visual Function

A total of 241 patients from 168 presumably unrelated families with a *PRPH2*-associated IRD were recruited at a median age of 56 years (range, 7–89 years). Age at symptom onset was available for 189 patients and 20 were asymptomatic at their last review. The median age at symptom onset was

Table 1. Clinical Characteristics of *PRPH2* Patients

Characteristics	*PRPH2* Cohort (n = 241)
Age at imaging (y) (n = 241)	
Mean ± SD	54.8 ± 15.5
Median (IQR)	55.8 (Q1, 44.9; Q3, 66.9)
Range	7–89
Sex (M:F)	118:123
Age at symptom onset (n = 189)	
Median (IQR)	40 (Q1, 30; Q3, 50)
Range	4–78
Last available VA in the right eye (n = 241)	
Median VA, in logMAR (IQR)	0.18 (Q1, 0; Q3, 0.54)
Median VA, in Snellen equivalent (IQR)	20/30 (Q1, 20/20; Q3, 20/80)
Last available VA in the left eye (n = 241)	
Median VA, in logMAR (IQR)	0.18 (Q1, 0; Q3, 0.42)
Median VA, in Snellen equivalent (IQR)	20/30 (Q1, 20/20; Q3, 20/60)
FAF, n/total (%)	
Normal	13/241 (5%)
BPD/VMD	27/241 (11%)
CACD	68/241 (28%)
PSPD	98/241 (41%)
RP	35/241 (15%)
ERG, no/total (%)	
Normal ffERG and PERG	8/100 (8%)
MD	21/100 (21%)
COD	16/100 (16%)
Cone-rod dystrophy	17/100 (17%)
Rod-cone dystrophy	38/100 (38%)

ffERG, full-field ERG.

40 years (IQR, 30–50 years; range, 4–78 years) (Table 1). The 20 asymptomatic patients were last reviewed at a median age of 39 years (range, 10–65 years). VA for the right and left eye was available for 241 patients. Median VA was 0.18 logMAR (IQR, 0–0.54 logMAR), or 20/30 Snellen equivalent (IQR, 20/20–20/80 Snellen equivalent) for the right eye, and 0.18 logMAR (IQR, 0–0.42 logMAR) or 20/30 Snellen equivalent (IQR, 20/20–20/60 Snellen equivalent) for the left eye. Although some interocular differences were large (−2.20 to +2.50), the mean VA between right and left eye was not significantly different (paired t test, $P = 0.11$).

Overall, VA showed stability until the fifth decade with a decline thereafter (Fig. 1). The proportion of patients with normal vision in their better seeing eye also declined with age (Fig. 1). Of 241 patients, 55 (22.8%) showed interocular asymmetry in VA greater than 0.3 logMAR. The 95% limits of agreements were −0.97 to +1.07 logMAR (Supplementary Material S1).

Fundus Autofluorescence

Of 241 *PRPH2* disease-associated variant carriers FAF was normal in 13 (5%), at a median age of 33 years (range, 7–71 years); of these 13 patients, 10 (77%) were asymptomatic (Fig. 2). Twenty-seven patients (11%) demonstrated a BPD (n = 21) or VMD (n = 6) FAF phenotype (Fig. 3), of which 3 (11%) were asymptomatic and the remaining 24 had a median age at symptom onset of 44 years (range, 26–70 years). The CACD FAF phenotype (Fig. 4) was observed in 68 patients (28%), with a median age at symptom onset of 40 years (range, 14–70 years) in 55 patients; 3 patients were asymptomatic (age, 13–55 years). PSPD (Fig. 5) was seen in 98 patients (41%) with a median age at symptom onset of 40 years (range, 7–78 years) in 73 patients; 4 patients were asymptomatic (range, 30–55 years). RP (Fig. 6) was observed in 35 patients (15%) with a median age at symptom onset of 33 years (range, 4–63 years) in 34 patients. Table 2 summarises the clinical features of each FAF phenotype. There were no significant difference in the sex distribution (P = 0.751). A younger age at imaging was observed in the normal FAF group ($P < 0.001$), which was likely a result of familial screening. Age at symptom onset was lower in the RP group as compared with BPD/VMD ($P = 0.048$) or PSPD ($P = 0.015$). VA in the better seeing eye was worse in the CACD group as compared with BPD/VMD (P = 0.035). An age-related decline in VA from the sixth decade was observed across all CACD, PSPD, and RP phenotype groups (Supplementary Material S2).

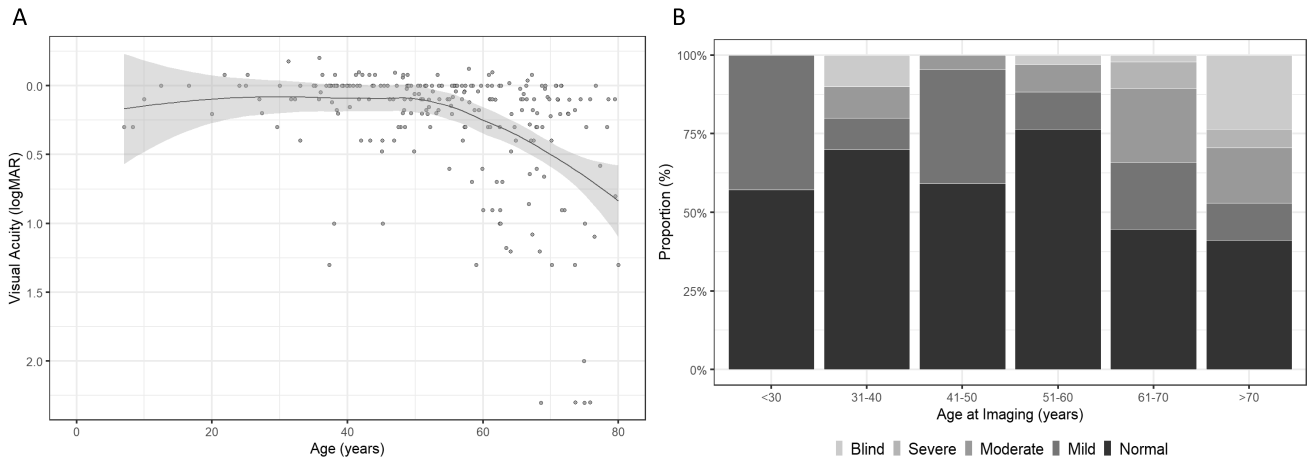

Figure 1. Locally estimated scatterplot smoothing (LOESS) curve using VA from the better-seeing eye illustrating the average evolution of VA with age across the entire cohort (**A**). Proportion (%) of *PRPH2* patients with normal, mild (VA, <20/40 and ≥20/60), moderate (VA, <20/60 and ≥20/200), severe visual impairment (VA, <20/200 and ≥20/400) and blindness (VA, <20/400) by age at imaging (**B**).

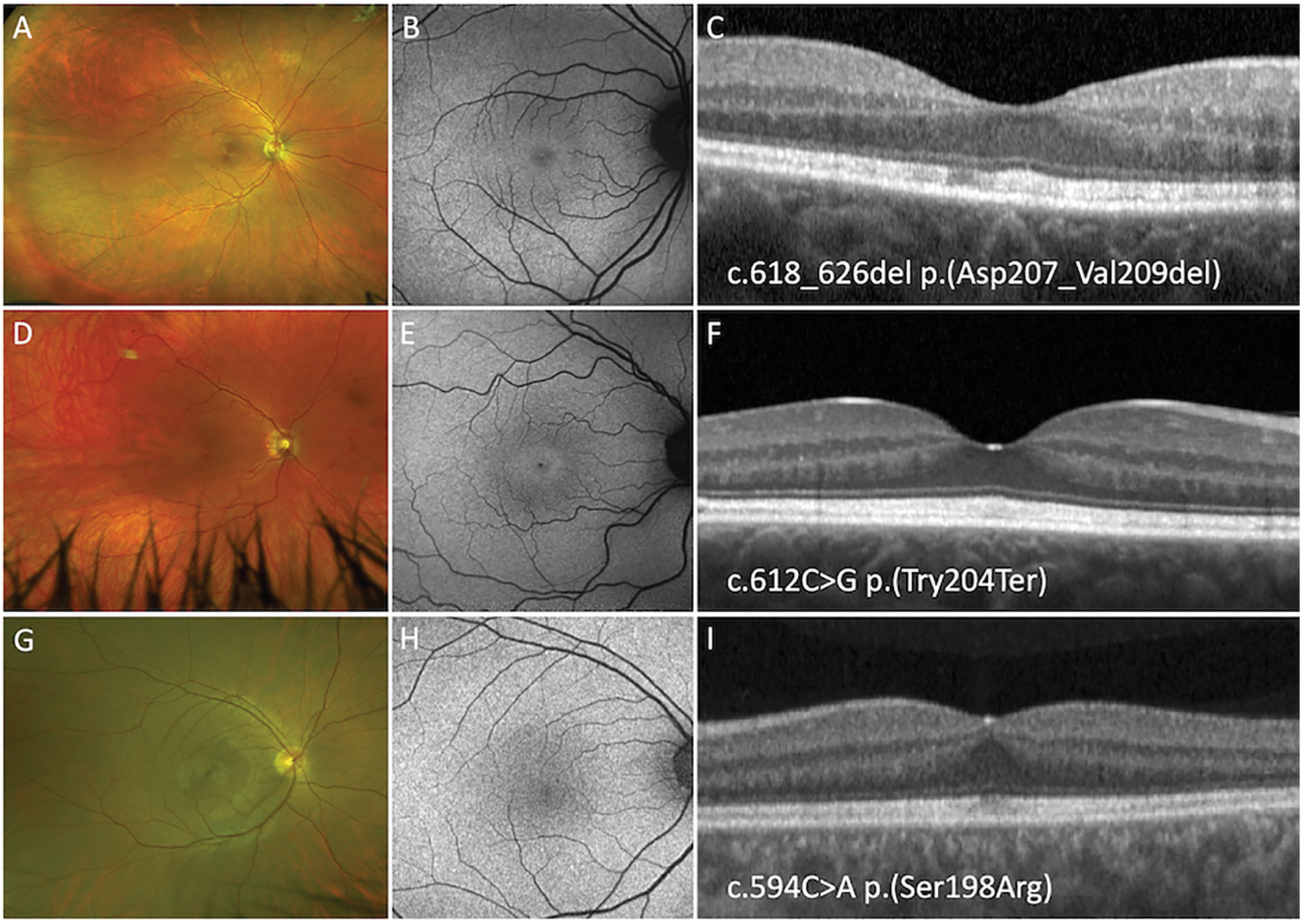

Figure 2. Optos pseudocolor, FAF, and SD-OCT imaging of a 40-year-old woman (**A**, **B**, **C**), a 39-year-old woman (**D**, **E**, **F**), and a 40 year-old-man (**G**, **H**, **I**) harboring the p.(Asp207_Val209del), p.(Try204Ter), and p.(Ser198Arg) *PRPH2* variants respectively. All three patients show normal pseudocolor and FAF imaging with thickening of band 2 on SD-OCT.

Electrophysiology

Full-field, pattern, and multifocal ERG (mfERG) data were available for 100 patients and this was performed at a median age of 52 years (range, 9–81 years). Of these patients, 29 (29%) had no generalized cone or rod dysfunction on full-field ERG. Of those remaining, 16 patients (16%) had isolated COD, 17 (17%) had CRD, and 38 (38%) had RCD (Table 2). Of the 29 patients with a normal full-field ERG, 26 had a PERG and 16 had a mfERG. Of those with a PERG, 8 (31%) were subnormal, whereas all 16 mfERG (100%) showed reduced response densities indicating macular dysfunction. Combining our PERG and mfERG data, 21 of 29 without generalized retinal dysfunction had evidence of localized macular dysfunction. Of the 12 with electrooculogram (EOG) and no generalized dysfunction on full-field ERG, 2 (16.7%) had a reduced Arden ratio (<1.7).[38] Of the 87 patients with detectable a- and b-waves with the DA3.0 response, 7 (8%) had a reduced b:a ratio (<1.2) in one or both eyes. In contrast, 31 patients (31%) had a reduced b:a ratio (<3.0) with the LA3.0 response in one or both eyes. Thus, this reduced b:a ratio was more frequently observed with the LA3.0 response as compared with DA3.0 (Supplementary Material S3). A cohort of controls (female:male ratio of 20:24) with a mean age of 54 years (range, 19–77 years) were enrolled from one site and tested with the RETIport 3.2 (Roland Consult, Brandenburg, Germany). Comparisons were made between the controls and the entire *PRPH2* cohort (Fig. 7). Information regarding the regression lines featured in Figures 7 and 8 is provided in Supplementary Material S3. Further comparisons were performed against a subset of *PRPH2* patients who were tested under the same conditions and at the same institution as the controls (Table 3, Supplementary Material S3).

Our *PRPH2* cohort showed a steeper decline in amplitude with age for both the DA0.01 and LA30 Hz when compared with controls (Fig. 7). The peak time was delayed in the LA30 Hz indicating cone system dysfunction. The a-wave in the DA3.0 and LA3.0 showed a greater age-related decline in the *PRPH2* group as compared with controls (Fig. 8). A delayed peak time was observed in the LA3.0 b-wave. A subanalysis at one Australian site between the *PRPH2* cohort and controls showed a significant difference in all DA and LA amplitude parameters ($P < 0.001$) with significant delays in the LA30 Hz and LA3.0 b-wave implicit times ($P < 0.001$) (Table 3). Of those exhibiting a normal or BPD/VMD FAF phenotype, most had a normal ERG or isolated macular dysfunction, whereas those with a PSPD or RP phenotype typically showed generalized rod and cone abnormalities (Table 2). Conversely, those with CACD had a varied elec-

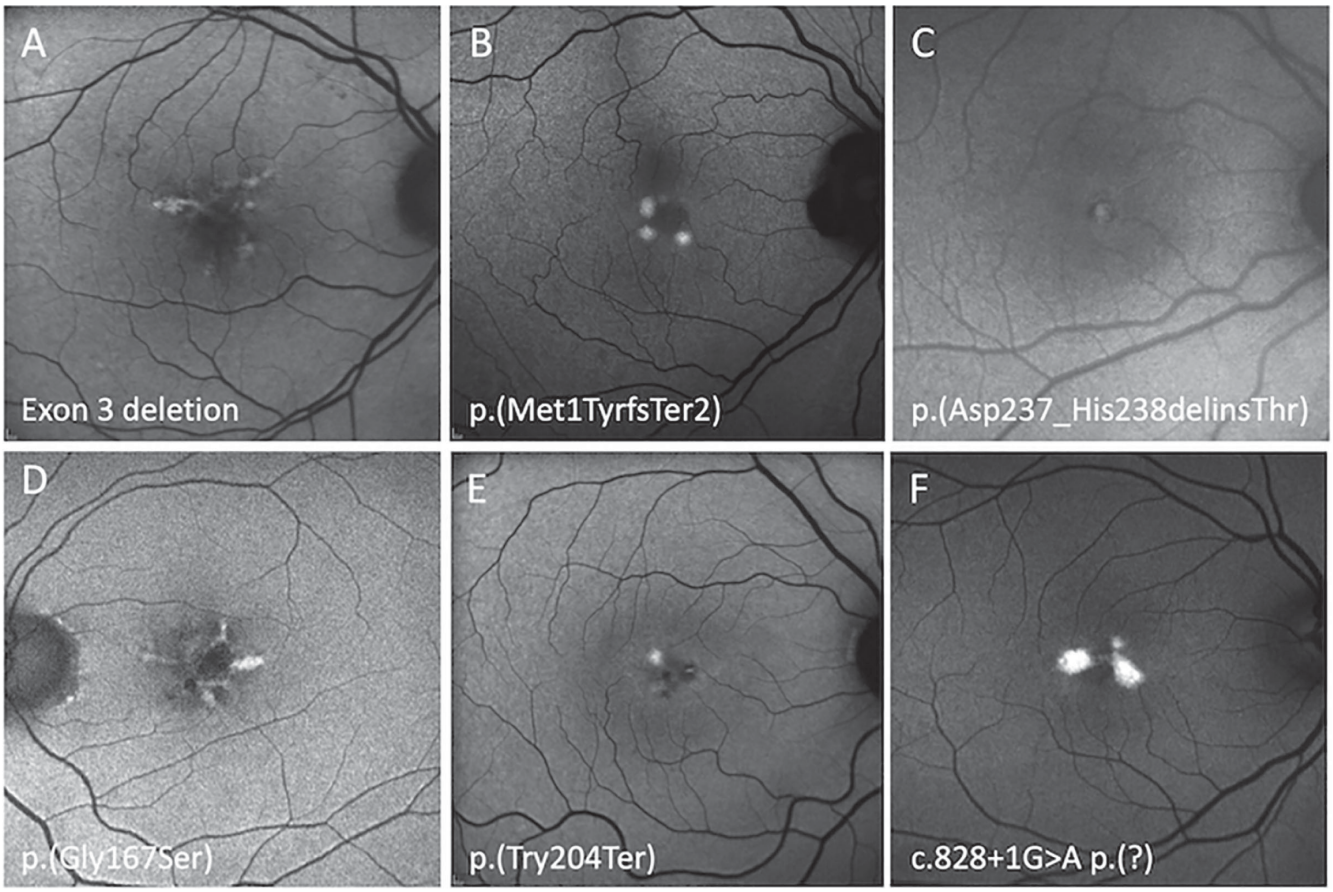

Figure 3. Optos FAF imaging of six *PRPH2* patients exhibiting focal central macula hyperautofluorescence defined as a BPD or VMD. An 88-year-old woman with a VA of 20/25 harboring exon 3 deletion (**A**), a 49-year-old woman with a VA of 20/20 harboring p.(Met1TyrfsTer2) (**B**), a 47-year-old woman with a VA of 20/16 harboring p.(Asp237_His238delinsThr) (**C**), a 66-year-old man with a VA of 20/25 harboring p.(Gly167Ser) (**D**), a 57-year-old woman with a VA of 20/20 harboring p.(Tyr204Ter) (**E**), and a 66-year-old woman with a VA of 20/25 harboring c.828+1G>A (**F**).

trophysiological phenotype ranging from a normal full-field and PERG ($n = 4$), MD ($n = 9$), COD ($n = 7$), to CRD ($n = 2$) (Supplementary Material S3).

Genetic Characteristics

Ninety-one unique variants were identified consisting of 46 missense, 5 inframe deletions, 21 frameshift, 12 nonsense, 2 exon deletions, 4 splice-site, and 1 start–loss. All variants were likely pathogenic or pathogenic based on American College of Medical Genetics criteria (Tables 4 and 5, Supplementary Material S4). Among the 46 missense variants at 36 codon positions, 5 amino acid substitutions at 5 codon positions and 1 inframe deletion–insertion were novel (Fig. 9, Supplementary Material S4). Sixteen of the 40 truncating or start–loss variants were also novel.

Of the 51 variants that altered protein sequence, 45 were localized to the D2 loop, whereas 1 resided in the N-terminal, 2 were in the transmembrane domain 1 (TMD1), and 3 were in the C-terminal (Fig. 9). The most common missense variants were at codon positions Arg172 ($n = 35$), Gly208 ($n = 16$), Gly167 ($n = 12$), and Glu178 ($n = 10$). There were 33 frameshift or nonsense variants occurring within exon 1 ($n = 20$), exon 2 ($n = 7$), and exon 3 ($n = 6$) that elicited a premature stop codon. The most common truncating variants occurred at positions Trp97Ter ($n = 9$), Tyr204Ter ($n = 8$), and Arg46Ter ($n = 7$) and at nucleotides c.394del p.(Gln132LysfsTer7) ($n = 6$) and c.259_266del p.(Asp87GlnfsTer87) ($n = 6$).

There were 71 patients with a CACD FAF phenotype carrying 13 missense variants at 10 codon positions. One of these missense variants p.(Ile196Asn) also manifested PSPD in one case and two cases with p.(Gly208Asp) and p.(Pro219Arg) had a normal FAF. In 85 patients with truncating, splice or start–loss variants, FAF phenotypes included PSPD (58%), BPD/VMD (21%), RP (16%), and normal (5%). The three most common frameshift and nonsense variants showed a similar FAF distribution (PSPD 57.5%, BPD/VMD 22.5%, RP 17.5%, and normal 2.5%). Notably, no truncating variants manifested a CACD phenotype. The three most common missense variants: p.(Tyr141Cys), p.(Gly167Ser) and p.(Glu178Arg) showed a similar FAF phenotype distribution (PSPD 67.7%, RP 22.6%, BPD/VMD 6.5%, and normal 3.2%). In-frame deletions appeared to be associated with a larger proportion of patients with a normal FAF (33% vs. 5%) and a lower frequency of PSPD as compared with truncating or null variants (33% vs. 58%).

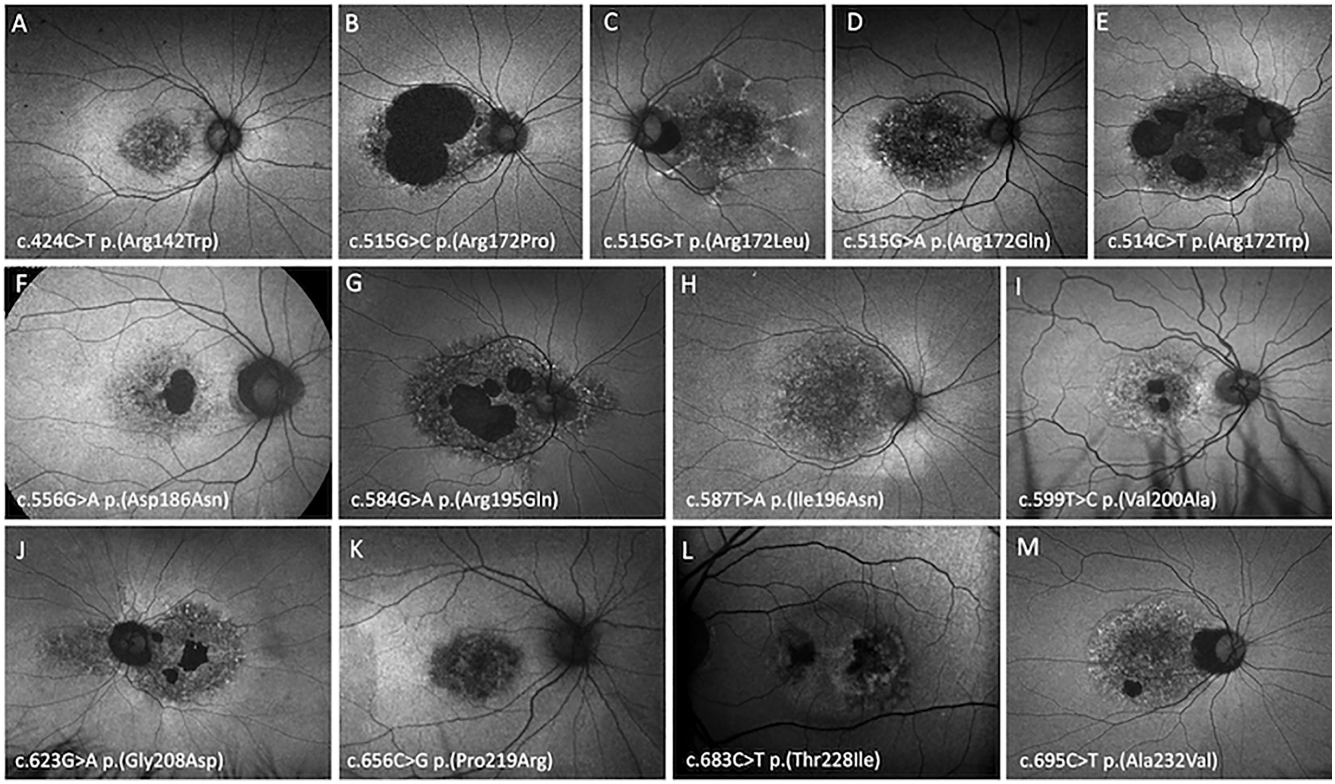

Figure 4. Optos FAF imaging of *PRPH2* patients demonstrating the CACD phenotype. A 53-year-old woman with VA of 20/25 harboring p.(Arg142Trp) (**A**), a 45-year-old man with a VA of 20/60 harboring p.(Arg172Pro) (**B**), an 89-year-old woman with a VA of 20/250 harboring p.(Arg172Leu) (**C**), a 46-year-old woman with a VA of 20/20 harboring p.(Arg172Gln) (**D**), a 67-year-old woman with a VA of 20/60 harboring p.(Arg172Trp) (**E**), a 33-year-old man with a VA of 20/20 harboring p.(Asp186Asn) (**F**), a 53-year-old man with a VA of 20/60 harboring p.(Arg195Gln) (**G**), a 27-year-old man with a VA of 20/40 harboring p.(Ile196Asn) (**H**), a 48-year-old man with a VA of counting fingers harboring p.(Val200Ala) (**I**), a 68-year-old man with a VA of 20/120 harboring p.(Gly208Asp) (**J**), a 61-year-old woman with a VA of 20/30 harboring p.(Pro219Arg) (**K**), a 61-year-old man with a VA of 20/15 harboring p.(Thr228Ile), (**L**) and a 53-year-old woman with a VA of 20/30 harboring p.(Ala232Val) (**M**).

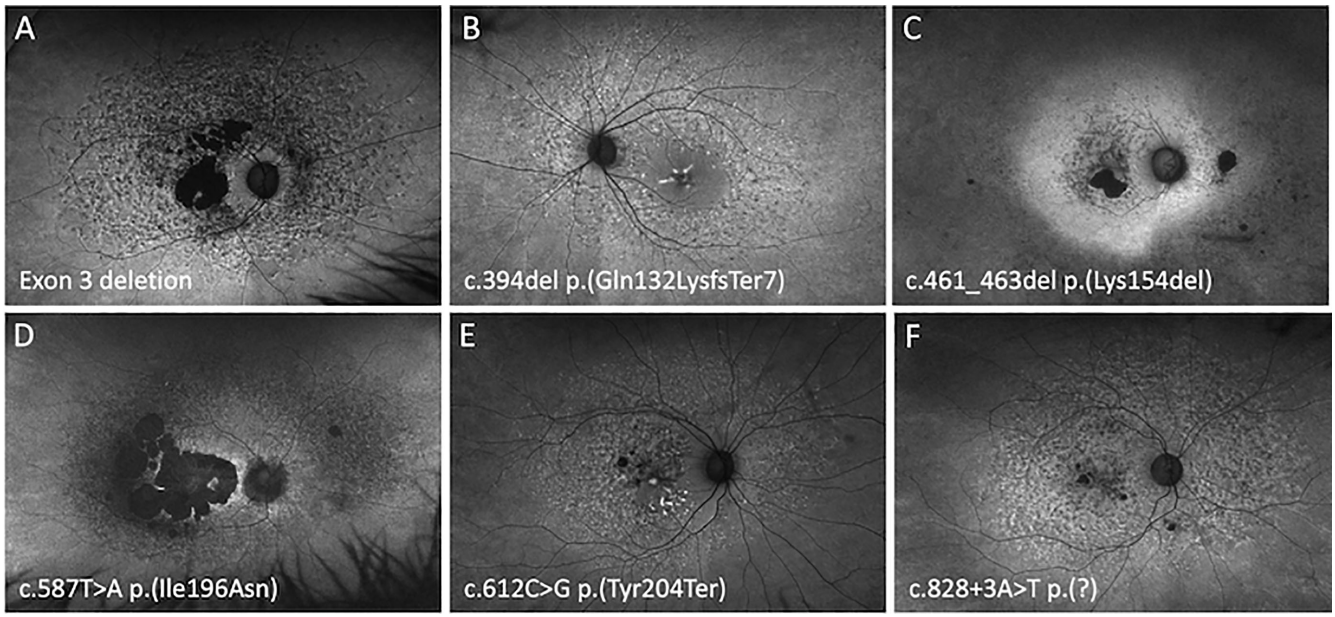

Figure 5. Optos FAF imaging of *PRPH2* patients demonstrating the PSPD phenotype. A 66-year-old woman with a VA of 20/200 harboring an exon 3 deletion (**A**), a 55-year-old woman with a VA of 20/80 harboring p.(Gln132LysfsTer7) (**B**), a 59-year-old woman with a VA of 20/20 harboring p.(Lys154del) (**C**), a 61-year-old woman with a VA of 20/40 harboring p.(Ile196Asn) (**D**), a 51-year-old woman with a VA of 20/20 harboring p.(Tyr204Ter) (**E**), and a 67-year-old woman with a VA of 20/90 harboring c.828+3A>T (**F**).

Investigative Ophthalmology & Visual Science

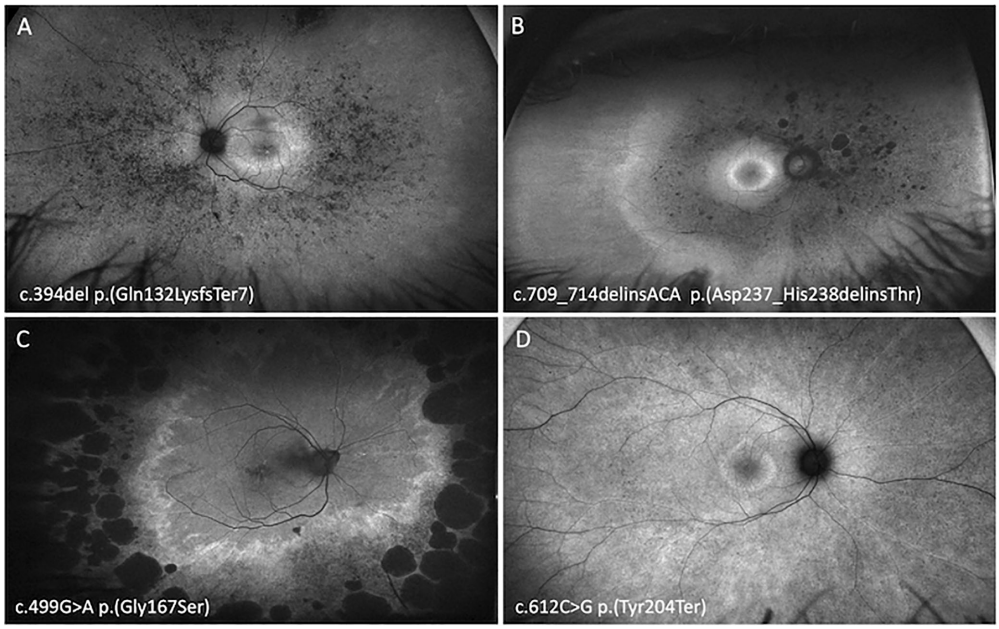

Figure 6. Optos FAF imaging of *PRPH2* patients demonstrating the RP phenotype. A 48-year-old woman with VA of 20/40 harboring p.(Gln132LysfsTer7) (**A**), a 55-year-old woman with a VA of 20/25 harboring p.(Asp237_His238delinsThr) (**B**), a 71-year-old woman with a VA of 20/30 harboring p.(Gly167Ser) (**C**), and a 36-year-old woman with a VA of 20/25 harboring p.(Tyr204Ter) (**D**).

Table 2. Clinical Characteristics of Each Phenotype Group

Phenotype Group	Normal	BPD/VMD	CACD	PSPD	RP	*P* Value
No. of cases	13	27	68	98	35	
Sex						
Female:male	7:6	17:10	35:35	48:50	18:17	0.751[a]
Age at imaging						
Mean ± SD	32 ± 17	56 ± 13	53 ± 16	60 ± 12	52 ± 15	< 0.001[†,‡]
Median (IQR)	33 (20–40)	56 (48–66)	54 (42–63)	61 (51–70)	52 (38–62)	
Asymptomatic count/total (%)	10/13 (77%)	3/27 (11%)	3/58 (5%)	4/77 (5%)	0/34 (0%)	
Age of symptom onset						
Mean ± SD	31 ± 34	45 ± 12	41 ± 13	44 ± 14	34 ± 17	0.004[†,§]
Median (IQR)	20 (13–45)	44 (40–51)	40 (34–50)	40 (35–53)	33 (20–48)	
Better eye VA (logMAR)						
Median (IQR)	0 (0–0.1)	0.02 (0–0.1)	0.2 (0–0.7)	0.1 (0–0.3)	0.1 (0–0.2)	0.002[‖,¶]
Electrophysiology						
Normal[*]	2	2	4	0	0	
Macular dystrophy	0	3	9	9	0	
Cone dystrophy	0	4	7	5	0	
Cone-rod dystrophy	0	0	2	15	0	
Rod-cone dystrophy	0	0	0	15	23	

[*] Normal full-field and PERG.
[a] χ^2 test.
[†] One-way ANOVA.
[‡] The normal group was significantly lower than all other groups (all $P < 0.001$). The PSPD group was significantly higher than both the CACD ($P = 0.012$) and RP ($P = 0.017$) groups.
[§] The RP group was younger than both BPD/VMD ($P = 0.048$) and PSPD ($P = 0.015$)
[‖] Kruskal–Wallis test.
[¶] VA for the BPD/VMD group was significantly lower than the CACD croup ($P = 0.035$)

Discussion

This large, international, multicenter study describes the clinical and genetic spectrum of 241 patients with 91 unique pathogenic or likely pathogenic *PRPH2* variants. Although the severity of *PRPH2*-associated IRD can vary considerably, VA often remained relatively stable until the fifth decade, with a constant decline thereafter. There was a range of retinal presentations including five distinct FAF phenotypes. Within each FAF phenotype group, there was often a spectrum of electrophysiological changes. Importantly, we observed 13 specific missense variants in the *PRPH2*

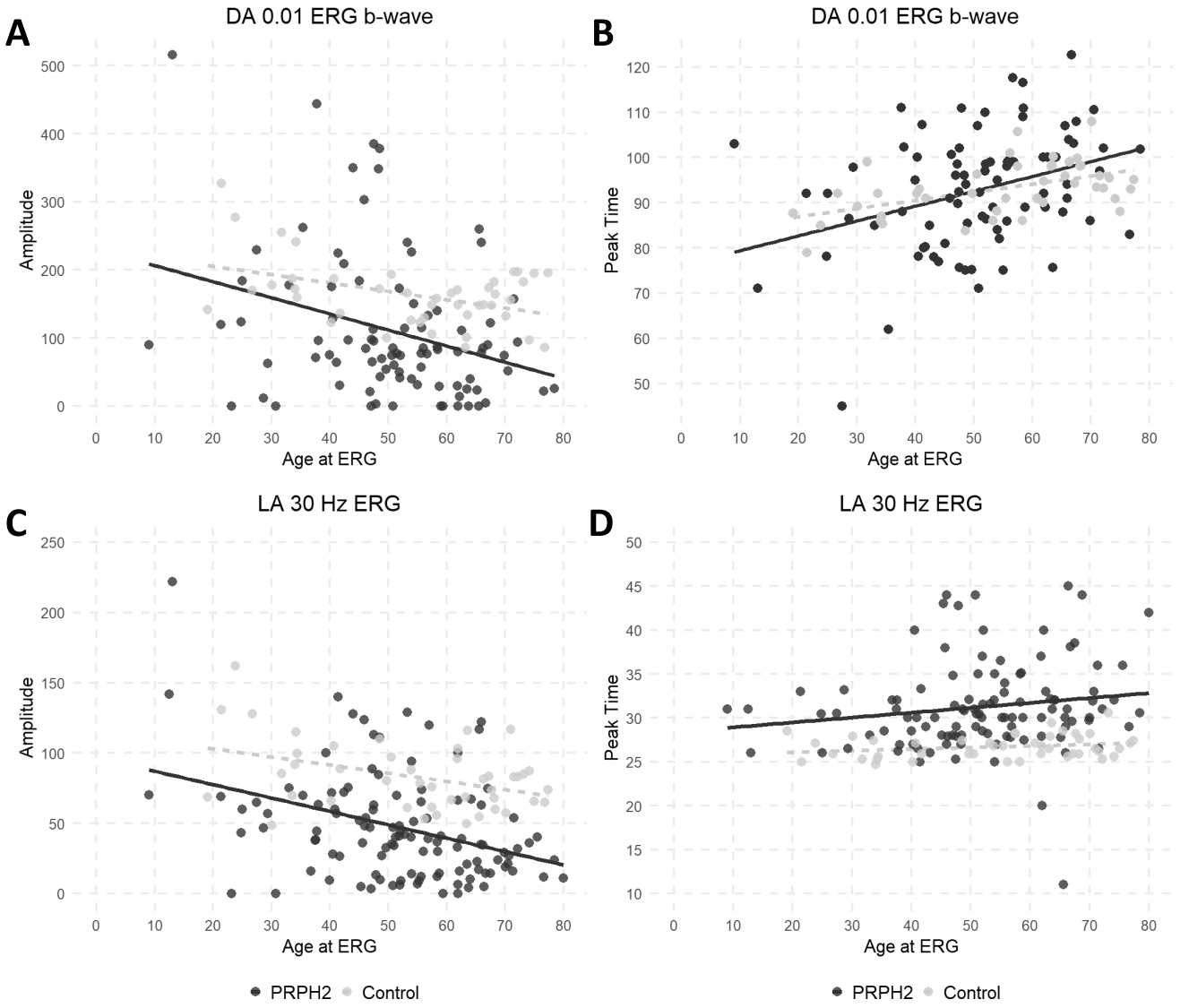

Figure 7. Scatter plots for electrophysiologic parameters and age. The full-field ERG component amplitudes and peak times in *PRPH2* patients (*black circles*) and unaffected controls (*grey circles*) are plotted against age. Data are shown for the DA 0.01 ERG (**A** and **B**), LA 30-Hz ERG (**C** and **D**). Regression lines are shown for the *PRPH2*-associated retinopathy (*solid line*) and control (*grey broken line*) data.

gene that were strongly associated with a CACD phenotype. Conversely truncating variants resulted in variable FAF phenotypes.

In previous *PRPH2* cohorts, clinical and electrophysiological terms have often been used without a clear distinction between their structural and functional associations.[9,25,39] Some studies classified patients as having a pattern dystrophy based on morphological features, including macular pigmentary changes in combination with functional features such as a normal or minimally abnormal full-field ERG.[9] In contrast, we classified patients into normal, BPD, VMD, PSPD, CACD, and RP groups based on their FAF pattern. We showed one FAF phenotype may have multiple ERG phenotypes and vice versa (Table 2). For example, PSPD was associated with MD (21%), COD (11%), CRD (34%), and RCD (34%) ERG phenotypes. Our observation of concurrent cone and rod dysfunction (68%) was like that reported by Boon et al. where one-half of the 17 patients with PSPD had cone and rod dysfunction.[40] Conversely, a COD was observed across the BPD, CACD, and PSPD FAF phenotypes groups. We observed a reduced b:a ratio in 8% and 31% of the rod and cone responses, respectively. This may be attributable to additional inner retinal dysfunction as previously described by Ba-Abbad et al.[41] The reduced b:a ratio in the DA3.0 response may also represent a predominance of DA cone responses with markedly reduced rods (manifesting as a photopic hill phenomenon in the dark). Thus, future studies need to incorporate the red DA3.0 and DA10.0 responses to look for DA cone responses and the photopic hill phenomenon, respectively.[42] This discordance between FAF and ERG phenotyping supports our proposal that clinicians should incorporate both standardized FAF and ERG grading systems. Because three ERG groups have been proposed in *ABCA4*-associated retinopathy,[43] future longitudinal studies should investigate the prognostic value of ERG grad-

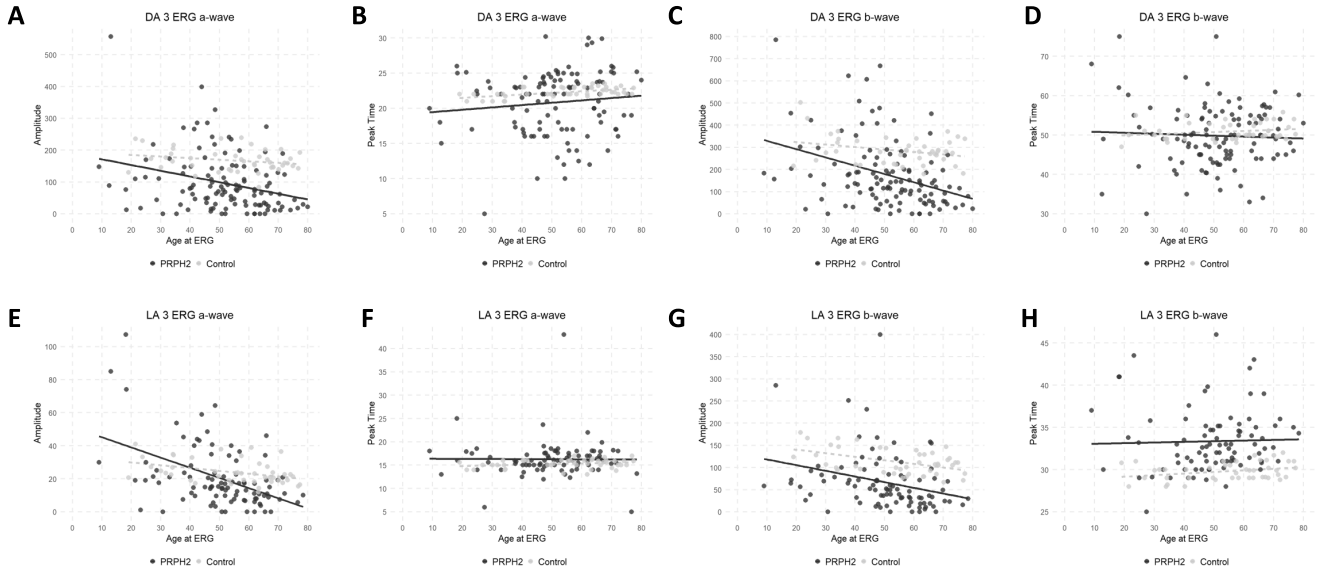

Figure 8. Scatter plots for electrophysiologic parameters and age. The major full-field ERG component amplitudes and peak times in *PRPH2* patients (*black circles*) and unaffected controls (*grey circles*) are plotted against age. Data are shown for the DA3.0 ERG a-wave (**A**, **B**) and b-wave (**C**, **D**), LA 3.0 ERG a-wave (**E**, **F**) and b-wave (**G**, **H**). Regression lines are shown for the *PRPH2*-associated retinopathy (*solid line*) and control (*grey broken line*) data.

Table 3. Amplitudes and Peak Times of the Full-Field ERG Components in a Control Group Compared With *PRPH2* at a Single Center

Stimulus	Component	Parameter	*PRPH2* $n = 25$ Median (5th, 95th)	Control $n = 44$ Median (5th, 95th)	*P* Value*
DA 0.01	b-wave	Amplitude peak time	81 (0, 349)	162 (97, 253)	<0.001
			94 (75, 110)	93 (85, 101)	1.000
DA 3.0	a-wave	Amplitude peak time	72 (0, 271)	163 (127, 235)	<0.001
			22 (13, 26)	22 (21, 23)	1.000
	b-wave	Amplitude peak time	137 (13, 466)	280 (211, 372)	<0.001
			50 (37, 62)	50 (48, 55)	1.000
LA 30-Hz	flicker	Amplitude peak time	39 (4, 123)	81 (53, 126)	<0.001
			30 (26, 42)	27 (25, 28)	<0.001
LA 3.0	a-wave	Amplitude peak time	15 (0, 56)	23 (16, 38)	0.003
			16 (13, 20)	15 (14, 17)	0.214
	b-wave	Amplitude peak time	52 (4, 168)	107 (77, 166)	<0.001
			33 (29, 41)	30 (28, 32)	<0.001

DA, dark adapted; LA, light adapted.
Amplitudes are in microvolts and peak times are in milliseconds. Statistical significance was established using the Mann–Whitney *U* test.
* Statistically significant after Bonferroni correction.

ing for predicting visual outcomes in *PRPH2*-asssociated IRD.

Of 91 different *PRPH2* variants, there were 21 frameshift, 12 nonsense, 2 exon deletions, 4 splice-site, and 1 start–loss, of which most were expected to result in loss of function or haploinsufficiency. Animal studies[44,45] suggest that haploinsufficiency affects rods more than cones, leading to RP. However, clinical case series have shown conflicting genotype–phenotype correlations. In a case series of 40 Japanese patients harboring 17 *PRPH2* variants, Oishi et al.[46] found no clear genotype–phenotype correlations. Reeves et al.[47] found an association of exon 1 variants with CRD, PSPD, and RP, whereas a pattern dystrophy was associated with variants in exon 2. Bianco et al.[9] observed that loss-of-function variants were associated with a mild pattern dystrophy and the addition of *ABCA4* variants resulted in a more severe phenotype. Peeters et al.[39] listed the missense variants exclusively associated with RP or a pattern dystrophy. In contrast with animal studies, we demonstrated a predominance of PSPD in more than one-half of these patients. This result was replicated in a subanalysis of 40 patients carrying the three most common truncating variants. Variable FAF phenotypes were observed in 73 patients with missense variants that were not associated with a CACD phenotype. The similar FAF phenotypic spectrum of these missense variants to truncating variants suggests these specific amino acid substitutions may lead to haploinsufficiency through retention or mislocalization of the PRPH2 protein to the photoreceptor inner segment.[48,49] Our observation that none of the 81 patients with truncating vari-

Table 4. Missense Variant List With In Silico Prediction and Phenotype

Codon	cDNA	Amino Acid	Exon	Protein Domain	PolyPhen2 Var	SIFT	REVEL	CADD	Mutation Taster	Grantham Score	Clinical Phenotype	ACMG Class	References
13	c.37C>T	p.Arg13Trp	1	NH2	Probably damaging (1.000)	Affect protein function (0.00)	0.502	25.3	Deleterious (88|12)	101	RP	5	Sohocki et al.[64]; Koyanagi et al.[65]; Peeters et al.[39]
38	c.112G>A	p.Gly38Arg	1	1st TM	Probably damaging (1.000)	Affect protein function (0.00)	0.876	26.6	Deleterious (81|19)	125	PSPD	4	Novel
41	c.122T>C	p.Leu41Pro	1	1st TM	Probably damaging (0.981)	Affect protein function (0.00)	0.916	27.3	Deleterious (77|23)	98	BPD	4	Peeters et al.[39]; Bianco et al.[9]
138	c.413T>G	p.Met138Arg	1	D2	Probably damaging (0.99)	Affect protein function (0.00)	0.856	27.5	Deleterious (85|15)	91	PSPD	4	Bianco et al.[9]
141	c.422A>G	p.Tyr141Cys	1	D2	Probably damaging (1.000)	Affect protein function (0.00)	0.881	29.3	Deleterious (86|14)	194	PSPD	5	Sohocki et al.[64]; Stone et al.[67]; Sullivan et al.[66]; Khani et al.[68]
142	c.424C>T	p.Arg142Trp	1	D2	Probably damaging (0.948)	Affect protein function (0.00)	0.635	25	Deleterious (74|26)	101	CACD	5	Hoyng et al.[10]; Klevering et al.[69]; Boon et al.[20]
153	c.457A>G	p.Lys153Glu	1	D2	Probably damaging (0.999)	Affect protein function (0.00)	0.864	28.3	Deleterious (89|11)	56	PSPD	5	Peeters et al.[39]
	c.458A>G	p.Lys153Arg	1	D2	Probably damaging (1.000)	Affect protein function (0.00)	0.828	27.8	Deleterious (85|15)	26	RP	5	Jacobson et al.[70]; Reeves et al.[47]; Peeters et al.[39]
167	c.499G>A	p.Gly167Ser	1	D2	Probably damaging (1.000)	Affect protein function (0.00)	0.953	28.8	Deleterious (84|16)	56	N; BPD; VMD; PSPD; RP	5	Testa et al.[71]; Coco-Martin et al.[72]
172	c.514C>T	p.Arg172Trp	1	D2	Probably damaging (0.967)	Affect protein function (0.00)	0.67	26	Deleterious (80|20)	101	CACD	5	Wells et al.[11]; Duncan et al.[73]; Reeves et al.[47]
	c.515G>A	p.Arg172Gln	1	D2	Benign (0.103)	Affect protein function (0.03)	0.453	26.6	Deleterious (64|36)	43	CACD	5	Wells et al.[11]; Wroblewski et al.[12]; Payne et al.[50]
	c.515G>C	p.Arg172Pro	1	D2	Possibly damaging (0.886)	Affect protein function (0.01)	0.63	27.3	Deleterious (57|43)	103	CACD	4	LOVD
	c.515G>T	p.Arg172Leu	1	D2	Possibly damaging (0.642)	Affect protein function (0.01)	0.491	26.8	Benign (45|55)	102	CACD	4	Novel
178	c.533A>G	p.Glu178Arg	1	D2	Probably damaging (0.978)	Affect protein function (0.00)	0.875	26.6	Deleterious (93|7)	43	PSPD; RP	5	Peeters et al.[39]
179	c.535T>G	p.Trp179Gly	1	D2	Probably damaging (0.999)	Affect protein function (0.00)	0.909	29.9	Deleterious (90|10)	184	RP	5	Colombo et al.[74]
185	c.554T>C	p.Leu185Pro	1	D2	Probably damaging (1.000)	Affect protein function (0.00)	0.915	29	Deleterious (98|2)	98	BPD	5	Peeters et al.[39]
186	c.556G>A	p.Asp186Asn	1	D2	Benign (0.124)	Affect protein function (0.00)	0.382	23.6	Deleterious (94|6)	23	CACD	4	Kohl et al.[13]; Martin-Merida et al.[75]; Almoguera et al.[76]
195	c.584G>A	p.Arg195Gln	2	D2	Probably damaging (0.978)	Affect protein function (0.00)	0.761	32	Deleterious (58|42)	43	CACD	5	Da Palma et al.[17]; Alapati et al.[51]
196	c.587T>A	p.Ile196Asn	2	D2	Possibly damaging (0.815)	Affect protein function (0.00)	0.306	29.4	Deleterious (61|39)	194	CACD; PSPD	5	Reeves et al.[47]; Peeters et al.[39]; Bianco et al.[9]
198	c.594C>A	p.Ser198Arg	2	D2	Probably damaging (0.999)	Affect protein function (0.00)	0.258	26.7	Deleterious (88|12)	110	N; PSPD; RP	4	Novel
	c.594C>G	p.Ser198Arg	2	D2	Probably damaging (0.983)	Affect protein function (0.00)	0.259	26.4	Deleterious (88|12)	110	RP	5	Sullivan et al.[66]; Manes et al.[77]; Peeters et al.[39]
200	c.599T>C	p.Val200Ala	2	D2	Benign (0.314)	Affect protein function (0.00)	0.281	28.9	Deleterious (80|20)	64	CACD	4	ClinVar, LOVD
208	c.623G>A	p.Gly208Asp	2	D2	Benign (0.206)	Affect protein function (0.03)	0.712	22.6	Deleterious (41|59)	94	N; CACD	4	Reeves et al.[47]; Bianco et al.[9]; Trujillo et al.[47]; Birtel et al.[58]

Table 4. Continued

Codon	cDNA	Amino Acid	Exon	Protein Domain	PolyPhen2 Var	SIFT	REVEL	CADD	Mutation Taster	Grantham Score	Clinical Phenotype	ACMG Class	References
209	c.625G>A	p.Val209Ile	2	D2	Probably damaging (0.998)	Affect protein function (0.00)	0.631	26.4	Benign (27|73)	29	RP	5	Coco-Martin et al.[72]
	c.625G>T	p.Val209Phe	2	D2	Probably damaging (1.000)	Affect protein function (0.00)	0.927	29.1	Deleterious (90|10)	50	PSPD	5	Carss et al.[78]; Peeters et al.[39]
210	c.628C>T	p.Pro210Ser	2	D2	Probably damaging (1.000)	Affect protein function (0.00)	0.928	28.7	Deleterious (92|8)	74	PSPD	5	Peeters et al.[39]
	c.629C>G	p.Pro210Arg	2	D2	Probably damaging (1.000)	Affect protein function (0.00)	0.89	27.5	Deleterious (95|5)	103	BPD	5	Boon et al.[20]; Duncan et al.[73]; Reeves et al.[47]
211	c.633C>A	p.Phe211Leu	2	D2	Probably damaging (0.997)	Affect protein function (0.00)	0.771	24.1	Deleterious (92|8)	22	RP	5	Ekstrom et al.[79]; Peeters et al.[39]
212	c.634A>C	p.Ser212Arg	2	D2	Probably damaging (1.000)	Affect protein function (0.00)	0.957	28.7	Deleterious (82|18)	110	PSPD	5	ClinVar
	c.635G>A	p.Ser212Asn	2	D2	Probably damaging (1.000)	Affect protein function (0.00)	0.797	28.5	Deleterious (70|30)	46	PSPD	4	Novel
	c.636C>G	p.Ser212Arg	2	D2	Probably damaging (1.000)	Affect protein function (0.00)	0.901	32	Deleterious (96|4)	110	N; PSPD	5	ClinVar
213	c.638G>A	p.Cys213Tyr	2	D2	Probably damaging (1.000)	Affect protein function (0.00)	0.946	31	Deleterious (100|0)	194	PSPD	5	Zhang et al.[80]; Duncan et al.[73]; Stone et al.[67]
214	c.642C>G	p.Cys214Trp	2	D2	Probably damaging (1.000)	Affect protein function (0.00)	0.874	27.7	Deleterious (99|1)	215	PSPD	5	Bianco et al.[9]
216	c.646C>T	p.Pro216Ser	2	D2	Possibly damaging (0.771)	Affect protein function (0.00)	0.682	25.5	Deleterious (81|19)	74	PSPD	5	Fishman et al.[81]; Stone et al.[67]; Coco-Martin et al.[72]
218	c.653C>G	p.Ser218Trp	2	D2	Probably damaging (0.999)	Affect protein function (0.00)	0.764	27.9	Deleterious (80|20)	177	BPD	4	Novel
219	c.656C>G	p.Pro219Arg	2	D2	Possibly damaging (0.713)	Affect protein function (0.00)	0.731	23.3	Deleterious (83|17)	103	N; CACD	5	Payne et al.[50]; Peeters et al.[39]
220	c.659G>A	p.Arg220Gln	2	D2	Probably damaging 0.987	Affect protein function (0.00)	0.724	31	Deleterious (85|15)	43	BPD; PSPD	5	Jacobson et al.[70]; Ellingford et al.[82];
	c.659G>C	p.Arg220Pro	2	D2	Probably damaging (0.993)	Affect protein function (0.00)	0.882	31	Deleterious (89|11)	103	PSPD	5	Reeves et al.[47]; Peeters et al.[39]
222	c.665G>C	p.Cys222Ser	2	D2	Possibly damaging (0.999)	Affect protein function (0.00)	0.918	29.1	Deleterious (95|5)	112	PSPD; RP	4	Ahmad et al.[83]; Liu et al.[84]; Peeter et al.[39]
228	c.683C>T	p.Thr228Ile	2	D2	Possibly damaging (0.776)	Affect protein function (0.00)	0.771	24.8	Deleterious (92|8)	89	CACD	4	Alapati et al.[51]; Reeves et al.[47]; Peeters et al.[39]
232	c.695C>T	p.Ala232Val	2	D2	Possibly damaging (0.871)	Affect protein function (0.00)	0.694	26.8	Deleterious (69|31)	64	CACD	4	ClinVar
246	c.738G>C	p.Trp246Cys	2	D2	Possibly damaging (0.986)	Affect protein function (0.00)	0.956	32	Deleterious (87|13)	215	RP	4	Manes et al.[77]; Peeters et al.[39]
250	c.749G>C	p.Cys250Ser	2	D2	Probably Damaging (1.000)	Affect protein function (0.00)	0.968	28.6	Deleterious (97|3)	112	PSPD	5	ClinVar
284	c.850C>G	p.Arg284Gly	3	COOH	Probably damaging (0.976)	Affect protein function (0.01)	0.753	26.2	Benign (41|59)	125	BPD	4	Bianco et al.[9]
289	c.866C>T	p.Ser289Leu	3	COOH	Possibly damaging (0.501)	Affect protein function (0.00)	0.212	24.5	Deleterious (69|31)	145	RP	5	de Breuk et al.[85]; Peeters et al.[39]
316	c.946T>G	p.Trp316Gly	3	COOH	Benign (0.031)	Tolerated (0.07)	0.157	22.7	Deleterious (67|33)	184	RP	4	Huang et al.[86]; Peeters et al.[39]

ACMG, American College of Medical Genetics; COOH, carboxyl terminus; D2, D2 loop; NH2, amine terminus; TM, transmembrane.

Table 5. Truncating and Start–Loss Variant List With Phenotype

Codon	Nucleotide Change	Protein Consequence	Mutation Type	Exon	Protein Domain	Phenotype	ACMG Class	References
	c.1A>T	p.Met1?	Start loss	1	N/A	PSPD	5	Peeters et al.[39]
	c.(828+1_829-1)_(*1_?)del	Exon 3 deletion	Exon deletion	3	N/A	BPD; PSPD	4	Novel
	deletion of exon 1	Exon 1 deletion	Exon deletion	1	N/A	N; PSPD	5	Novel
	c.582-1G>A	p.(?)	Splicing	intron 1	N/A	PSPD	5	Reeves et al.[47]; Bianco et al.[9]
	c.828+1G>A	p.(?)	Splicing	intron 2	N/A	BPD	5	Peeters et al.[39]
	c.828+2T>C	p.(?)	Splicing	intron 2	N/A	PSPD	5	Peeters et al.[39]
	c.828+3A>T	p.(?)	Splicing	intron 2	N/A	PSPD	5	Peeters et al.[39]; Sullivan et al.[94]
46	c.136C>T	p.Arg46Ter	Nonsense	1	D1	BPD; PSPD; RP	5	Bianco et al.[9]
97	c.290G>A	p.Trp97Ter	Nonsense	1	C	BPD; VMD; PSPD; RP	5	Bianco et al.[9]
97	c.291G>A	p.Trp97Ter	Nonsense	1	3rd TM	N	4	Novel
126	c.372_381de linsAAGCTGA	p.Leu126Ter	Nonsense	1	D2	N	4	LOVD
179	c.536G>A	p.Trp179Ter	Nonsense	1	D2	RP	4	LOVD
191	c.571G>T	p.Glu191Ter	Nonsense	1	D2	PSPD; RP	5	Birtel et al.[58]; Duncker et al.[95]; Peeters et al.[39]
195	c.583C>T	p.Arg195Ter	Nonsense	2	D2	PSPD	5	Peeters et al.[39]; Alapati et al.[51]
197	c.589A>T	p.Lys197Ter	Nonsense	2	D2	PSPD	4	Novel
204	c.612C>G	p.Tyr204Ter	Nonsense	2	D2	N; BPD; PSPD; RP	5	Birtel et al.[58]; Peeters et al.[39]
236	c.708C>A	p.Tyr236Ter	Nonsense	2	D2	PSPD	5	Novel
257	c.771_772delinsGA	p.Tyr257Ter	Nonsense	2	D2	PSPD	4	Bianco et al.[9]
300	c.897dup	p.Glu300Ter	Nonsense	3	COOH	BPD	4	Novel
1	c.1_7del	p.Met1TyrfsTer2	Frameshift	1	NH2	BPD; PSPD; RP	4	Novel
12	c.33del	p.Lys12SerfsTer12	Frameshift	1	1st TM	BPD	5	Novel
23	c.68del	p.Met23ArgfsTer15	Frameshift	1	1st TM	VMD; PSPD	4	Bianco et al.[9]
25	c.73_74del	p.Trp25ValfsTer19	Frameshift	1	1st TM	VMD; PSPD	5	Kajiwara et al.[87]
38	c.113del	p.Gly38AspfsTer4	Frameshift	1	1st TM	BPD	5	Yang et al.[88]; Reeves et al.[47]
42	c.115delinsTTGTTCCT	p.Lys42ValfsTer5	Frameshift	1	D1	PSPD	4	Novel
60	c.172_176dup	p.Val60IlefsTer7	Frameshift	1	2nd TM	PSPD	5	Novel
72	c.212_213insAT	p.Cys72SerfsTer28	Frameshift	1	C	RP	4	Novel
87	c.259_266del	p.Asp87GlnfsTer87	Frameshift	1	D2	PSPD	5	Reeves et al.[47]; Carss et al.[78]
132	c.394del	p.Gln132LysfsTer7	Frameshift	1	D2	VMD; PSPD; RP	5	Boon et al.[40]
147	c.440del	p.Pro147LeufsTer6	Frameshift	1	D2	PSPD	4	Novel
148	c.441del	p.Gly148AlafsTer5	Frameshift	1	D2	PSPD	5	Kajiwara et al.[87]; Boon et al.[40]; Birtel et al.[58]
156	c.468_481delinsG	p.Ile156MetfsTer96	Frameshift	1	D2	PSPD	4	Novel
193	c.578_579del	p.Lys193ArgfsTer24	Frameshift	1	D2	BPD	5	Birtel et al.[58]
216	c.646_649delinsGG	p.Pro216GlyfsTer84	Frameshift	2	COOH	PSPD	5	Reeves et al.[47]
236	c.702_706dup	p.Tyr236SerfsTer22	Frameshift	2	D2	PSPD	4	Bianco et al.[9]
246	c.734dup	p.Trp246ValfsTer55	Frameshift	3	COOH	PSPD	4	Sodi et al.[89]
301	c.903del	p.Ser301ArgfsTer23	Frameshift	3	COOH	RP	4	Novel
304	c.910_911insG	p.Gln304ArgfsTer88	Frameshift+Elong	3	COOH	RP	4	Novel
315	c.943dup	p.Thr315AsnfsTer77	Frameshift+Elong	3	COOH	RP	4	Novel
322	c.964_965del	p.Ser322CysfsTer69	Frameshift+Elong	3	COOH	PSPD	4	Reeves et al.[47]
154	c.461_463del	p.Lys154del	Inframe deletion	1	D2	PSPD	5	Weleber et al.[90]
169	c.505_507del	p.Asn169del	Inframe deletion	1	D2	PSPD	5	van Lith-Verhoeven et al.[91]
207	c.618_626del	p.Asp207_Val209del	Inframe deletion	2	D2	N; RP	5	Kalyanasundaram et al.[92]
237	c.709_714delinsACA	p.Asp237_His238 delinsThr	Inframe deletion	2	D2	N: VMD: RP	4	Novel
271	c.811_813del	p.Leu271del	Inframe deletion	2	D2	N; PSPD; RP	5	Jin et al.[93]

ACMG, American College of Medical Genetics; COOH, carboxyl terminus; D2, D2 loop; NH2, amine terminus; TM, transmembrane.

ants demonstrated a CACD FAF phenotype warrants further consideration.

CACD was observed in 71 patients harboring 13 missense variants at 10 codon positions. Nearly all of these variants exhibited a CACD phenotype with the exception of p.(Ile196Asn), which also manifested as a PSPD in one patient. Before this paper the CACD phenotype had only been associated with missense variants at five codon positions. The p.(Pro219Arg) and p.(Thr228Ile) variants have been reported with a macular and pattern dystrophy respectively, despite no FAF imaging.[50,51] Similarly, p.(Asp186Asn) was reported to manifest a CRD and RP phenotype without supportive FAF imaging.[13] Although substitutions at Arg172 to Trp or Gln have been described, p.(Arg172Pro) and p.(Arg172Leu) have not been reported previously to cause CACD. Despite previous reports suggesting truncating *PRPH2* variants can cause CACD, we propose CACD only presents with specific missense

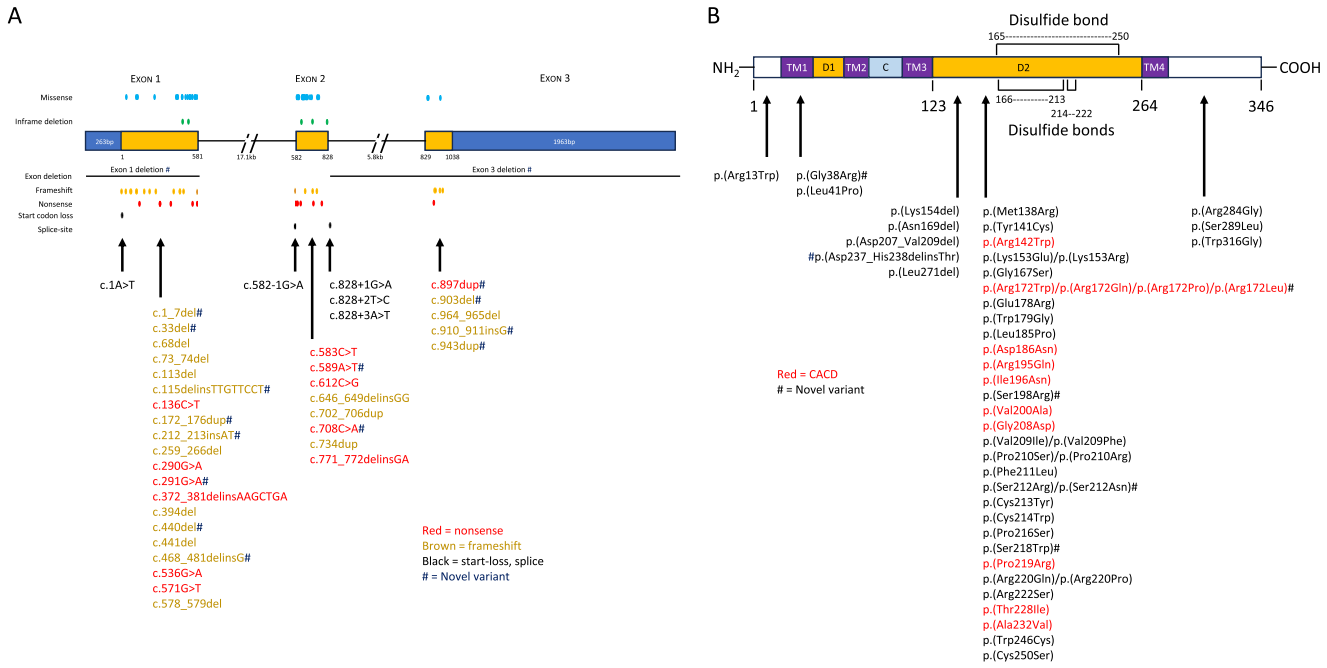

Figure 9. Position and type of *PRPH2* truncating variants (nonsense, frameshift, start-loss, splice site) by exon location (**A**). Missense and inframe deletion variants and their protein positions within our *PRPH2* cohort (**B**).

variants. Antonelli et al.[25] described a case of CACD with p.(Trp246ValfsTer55). FAF imaging, however, was atypical, demonstrating central macular hypoautofluorescence, and hyperautofluorescence fleck-like deposits that extended beyond the vascular arcades. Daftarian et al.[52] described p.(Gln239Ter) to be associated with CACD. Their FAF imaging, however, was more suggestive of a PSPD. To date, Boon et al.[20] have published the largest case series of CACD including 103 patients, most of whom carried the p.(Arg142Trp) variant. Other *PRPH2* variants, including p.(Arg172Trp),[53–55] p.(Arg172Gln),[53,12] p.(Arg195Gln),[17,51] p.(Arg195Leu),[14,15,56] p.(Asp196Asn),[9,39,47] p.(Arg203Pro),[16] and p.(Gly208Asp)[13,57,58] have also been associated with CACD. Nonpenetrance has been associated with p.(Arg172Trp) up to the age of 24.[5] Full penetrance was initially described with p.(Arg142Trp); however, Boon et al.[4] later described three families with evidence of nonpenetrance. In our cohort, two cases with normal FAF harbored the p.(Gly208Asp) and p.(Pro219Arg) variants; the former was reported previously to have incomplete penetrance.[59] Both variants were also shown to exhibit a CACD phenotype in this study. We found some carriers may remain asymptomatic up to 69 years of age. Within our cohort, nonpenetrance, defined as an absence of macular abnormalities on fundus color or FAF imaging, was seen in nearly 6% of patients (13/241) and observed up to 71 years of age. In contrast, Boon et al.[4] proposed nonpenetrance may be up to 21% in CACD-specific variants; however, this estimate may not be generalizable to our cohort. Finally, a knock-in animal model of CACD due to p.(Arg195Leu) demonstrated a progressive decrease in VA and ERG amplitudes in both scotopic and photopic conditions.[60] Our ERG data for CACD showed a similar trend toward greater cone than rod involvement as reported previously by Hoyng and Deutman.[19] It is intriguing that these animals exhibited evidence of disrupted communication between photoreceptors, bipolar and horizontal cells, supporting the observation of a reduced b:a ratio.

The current study is subject to the known limitations of retrospective clinical data entry, such as missing data and variable protocols, as well as devices used for VA, FAF, and ERG acquisition. A prior study described discordance in VA derived from a Snellen chart compared with a logMAR chart.[61] Thus, any observed trend in VA should be interpreted with caution. Future prospective studies using a standardized VA measurement will reduce this bias. An analysis of age-related changes in VA, FAF and ERG was not possible owing to an absence of longitudinal data. Examination of the ERG waveforms for the DA10.0 response would have been useful to elucidate the presence of the photopic hill phenomenon given the reduced b:a ratio we observed in the DA3.0. In addition, we did not include juxtafoveal lesions as part of the CACD spectrum, because these were often difficult to differentiate from VMD and BPD FAF phenotypes. Future prospective studies with structural and functional parameters will enhance our current knowledge of disease progression and provide more reliable and standardized biomarkers for tracking *PRPH2* disease progression.[62,63]

This study found a large variability in VA, FAF, and ERG phenotypes in patients with molecularly confirmed pathogenic or likely pathogenic variants in the *PRPH2* gene. We observed significant discordance between FAF and ERG phenotypes. To our knowledge, this work represents the largest *PRPH2* cohort with multimodal imaging. We report a novel genotype–phenotype correlation whereby patients harboring 13 missense variants at 10 codon positions predominately manifested a CACD phenotype. Additional studies, including cellular disease models of CACD-specific variants and longitudinal evaluation with prospective data, are still required. The detailed clinical and genetic information provided here will be useful for clinicians to

aid their work-up of patients with a *PRPH2*-associated IRD.

Acknowledgments

Disclosure: **R.C. Heath Jeffery**, None; **J.A. Thompson**, Retina Australia; **J. Lo**, None; **E.S. Chelva**, None; **S. Armstrong**, None; **J.S. Pulido**, None; **R. Procopio**, None; **A.L. Vincent**, None; **L. Bianco**, None; **M. Battaglia Parodi**, None; **L. Ziccardi**, None; **G. Antonelli**, None; **L. Barbano**, None; **J.P. Marques**, None; **S. Geada**, None; **A. L. Carvalho**, None; **W. Chao Tang**, None; **C. Mun Chan**, None; **C.J.F. Boon**, None; **J. Hensman**, None; **T.-C. Chen**, None; **C.-Y. Lin**, None; **P.-L. Chen**, None; **A. Vincent**, None; **A. Tumber**, None; **E. Heon**, None; **J.R. Grigg**, NHMRC APP1116360, APP1099165, APP1109056; **R.V. Jamieson**, NHMRC APP1116360, APP1099165, APP1109056; **E.E. Cornish**, None; **B.M. Nash**, None; **S. Borooah**, Foundation Fighting Blindness Grant CD-GT-0918-0746-SEI and Nixon Visions Foundation; **L.N. Ayton**, Novartis, Apellis, National Health & Medical Research Council (NHMRC) GNT1195713; **A.C. Britten-Jones**, None; **T.L. Edwards**, None; **J.B. Ruddle**, None; **A. Sharma**, None; **R.G. Porter**, None; **T.M. Lamey**, Retina Australia; **T.L. McLaren**, Retina Australia; **S. McLenachan**, None; **D. Roshandel**, None; **F.K. Chen**, Future Health Research and Innovation Fund, the McCusker Charitable Foundation, Channel 7 Telethon Trust, Retina Australia, NHMRC GNT1116360, GNT1188694, GNT1054712 and MRF1142962

References

1. Heath Jeffery RC, Mukhtar SA, McAllister IL, et al. Inherited retinal diseases are the most common cause of blindness in the working-age population in Australia. *Ophthalmic Genet*. 2021;42(4):431–439.
2. Pontikos N, Arno G, Jurkute N, et al. Genetic basis of inherited retinal disease in a molecularly characterized cohort of more than 3000 families from the United Kingdom. *Ophthalmology*. 2020;127(10):1384–1394.
3. Stenson PD, Mort M, Ball EV, Shaw K, Phillips A, Cooper DN. The human gene mutation database: building a comprehensive mutation repository for clinical and molecular genetics, diagnostic testing and personalized genomic medicine. *Hum Genet*. 2014;133(1):1–9.
4. Boon CJ, den Hollander AI, Hoyng CB, Cremers FP, Klevering BJ, Keunen JE. The spectrum of retinal dystrophies caused by mutations in the peripherin/RDS gene. *Prog Retina Eye Res*. 2008;27(2):213–235.
5. Michaelides M, Holder GE, Bradshaw K, Hunt DM, Moore AT. Cone-rod dystrophy, intrafamilial variability, and incomplete penetrance associated with the R172W mutation in the peripherin/RDS gene. *Ophthalmology*. 2005;112(9), 1592–1598.
6. Ikelle L, Makia M, Lewis T, et al. Comparative study of PRPH2 D2 loop mutants reveals divergent disease mechanism in rods and cones. *Cell Mol Life Sci*. 2023;80(8):214.
7. Poloschek CM, Bach M, Lagrèze WA, et al. ABCA4 and ROM1: implications for modification of the PRPH2-associated macular dystrophy phenotype. *Invest Ophthalmol Vis Sci*. 2010;51(8):4253–4265.
8. Leroy BP, Kailasanathan A, De Laey JJ, Black GC, Manson FD. Intrafamilial phenotypic variability in families with RDS mutations: Exclusion of ROM1 as a genetic modifier for those with retinitis pigmentosa. *Br J Ophthalmol*. 2007;91(1):89–93.
9. Bianco L, Arrigo A, Antropoli A, et al. PRPH2-associated retinopathy: novel variants and genotype-phenotype correlations. *Ophthalmol Retina*. 2023;7(5):450–461.
10. Hoyng CB, Heutink P, Testers L, Pinckers A, Deutman AF, Oostra BA. Autosomal dominant central areolar choroidal dystrophy caused by a mutation in codon 142 in the peripherin/RDS gene. *Am J Ophthalmol*. 1996;121(6):623–629.
11. Wells J, Wroblewski J, Keen J, et al. Mutations in the human retinal degeneration slow (RDS) gene can cause either retinitis pigmentosa or macular dystrophy. *Nat Genet*. 1993;3(3):213–218.
12. Wroblewski JJ, Wells JA, 3rd, Eckstein A, et al. Macular dystrophy associated with mutations at codon 172 in the human retinal degeneration slow gene. *Ophthalmology*. 1994;101(1):12–22.
13. Kohl S, Christ-Adler M, Apfelstedt-Sylla E, et al. RDS/peripherin gene mutations are frequent causes of central retinal dystrophies. *J Med Genetics*. 1997;34(8):620–626.
14. Yanagihashi S, Nakazawa M, Kurotaki J, Sato M, Miyagawa Y, Ohguro H. Autosomal dominant central areolar choroidal dystrophy and a novel Arg195Leu mutation in the peripherin/RDS gene. *Arch Ophthalmol*. 2003;121(10):1458–1461.
15. Keilhauer CN, Meigen T, Weber BH. Clinical findings in a multigeneration family with autosomal dominant central areolar choroidal dystrophy associated with an Arg195Leu mutation in the peripherin/RDS gene. *Arch Ophthalmol*. 2006;124(7):1020–1027.
16. Choi H, Cloutier A, Lally D. PRPH2-associated macular dystrophy in 4 family members with a novel mutation. *Ophthalmic Genet*. 2022;43(2):235–239.
17. Da Palma MM, Martin D, Salles MV, et al. Retinal dystrophies and variants in PRPH2. *Arq Bras Oftalmol*. 2019;82(2):158–160.
18. Marques JP, Carvalho AL, Henriques J, et al. Design, development and deployment of a web-based interoperable registry for inherited retinal dystrophies in Portugal: the IRD-PT. *Orphanet J Rare Dis*. 2020;15(1):304.
19. Hoyng CB, Deutman AF. The development of central areolar choroidal dystrophy. *Graefes Arch Clin Exp Ophthalmol*. 1996;234(2):87–93.
20. Boon CF, Klevering JB, Cremers FPM, et al. Central areolar choroidal dystrophy. *Ophthalmology*. 2009;116(4):771–782.
21. Robson AG, Frishman LJ, Grigg J, et al. ISCEV Standard for full-field clinical electroretinography (2022 update). *Doc Ophthalmol*. 2022;144:165–177.
22. Bach M, Brigell M, Hawlina M, et al. ISCEV standard for clinical pattern electroretinography (PERG) - 2012 update. *Doc Ophthalmol*. 2013;126:1–7.
23. Hood D, Bach M, Brigell M, et al. ISCEV Standard for clinical multifocal electroretinography (2011 edition). *Doc Ophthalmol*. 2012;124:1–13.
24. Heath Jeffery RC, Thompson JA, Lamey TM, et al. Longitudinal analysis of functional and structural outcome measures in PRPH2-associated retinal dystrophy. *Ophthalmol Retina*. 2023;7(1):81–91.
25. Antonelli G, Parravano M, Barbano L, et al. Multimodal study of PRPH2 gene-related retinal phenotypes. *Diagnostics (Basel)*. 2022;12(8):1851.
26. Richards S, Aziz N, Bale S, et al. Standards and guidelines for the interpretation of sequence variants: a joint consensus recommendation of the American College of Medical Genetics and Genomics and the Association for Molecular Pathology. *Genet Med*. 2015;17(5):405–424.
27. Abou Tayoun AN, Pesaran T, DiStefano MT, et al. Recommendations for interpreting the loss of function PVS1 ACMG/AMP variant criterion. *Hum Mutat*. 2018;39(11):1517–1524.
28. Adzhubei IA, Schmidt S, Peshkin L, et al. A method and server for predicting damaging missense mutations. *Nat Methods*. 2010;7(4):248–249.

Investigative Ophthalmology & Visual Science

29. Ng PC, Henikoff S. Predicting deleterious amino acid substitutions. *Genome Res*. 2001;11(5):863–874.
30. Ioannidis NM, Rothstein JH, Pejaver V, et al. REVEL: an ensemble method for predicting the pathogenicity of rare missense variants. *Am J Hum Genet*. 2016;99(4):877–885.
31. Kircher M, Witten DM, Jain P, O'Roak BJ, Cooper GM, Shendure J, A general framework for estimating the relative pathogenicity of human genetic variants. *Nat Genet*. 2014;46(3):310–315.
32. Hu J, Ng PC. SIFT Indel: predictions for the functional effects of amino acid insertions/deletions in proteins. *PLoS One*. 2013;8(10):e77940.
33. Hu J, Ng PC. Predicting the effects of frameshifting indels. *Genome Biol*. 2012; 13(2):R9.
34. Douville C, Masica DL, Stenson PD, et al. Assessing the pathogenicity of insertion and deletion variants with the Variant Effect Scoring Tool (VEST-Indel). *Hum Mutat*. 2016;37(1):28–35.
35. Schwarz JM, Rodelsperger C, Schuelke M, Seelow D. MutationTaster evaluates disease-causing potential of sequence alterations. *Nat Meth*. 2010;7(8):575–576.
36. Zhou H, Gao M, Skolnick J. ENTPRISE-X: predicting disease-associated frameshift and nonsense mutations. *PLoS One*. 2018;13(5):e0196849.
37. Jaganathan K, Kyriazopoulou Panagiotopoulou S, et al. Predicting splicing from primary sequence with deep learning. *Cell*. 2019;176(3):535–548.e24.
38. Constable PA, Bach M, Frishman LJ; for the International Society for Clinical Electrophysiology of Vision; ISCEV standard for clinical electro-oculography (2017 update). *Doc Ophthalmol*. 2017;134(1):1–9.
39. Peeters MHC, Khan M, Rooijakkers AAMB, et al. PRPH2 mutation update: in silico assessment of 245 reported and 7 novel variants in patients with retinal disease. *Hum Mutat*. 2021; 42(12):1521–1547.
40. Boon CJF, van Schooneveld MJ, den Hollander AI, et al. Mutations in the peripherin/RDS gene are an important cause of multifocal pattern dystrophy simulating STGD1/fundus flavimaculatus. *Br J Ophthalmol*. 2007;91:1504–1511.
41. Ba-Abbad R, Robson AG, Yap YC, et al. Prph2 mutations as a cause of electronegative ERG. *Retina*. 2014;34(6):1235–1243.
42. Holder GE, Mahroo O. Electronegative ERG or pseudonegative ERG? *Doc Ophthalmol*. 2022;145(3):283–286.
43. Lois N, Holder GE, Bunce C, Fitzke FW, Bird AC. Phenotypic subtypes of Stargardt macular dystrophy—fundus flavimaculatus. *Arch Ophthalmol*. 2001;119(3):359–369.
44. Stricker HM, Ding X, Quiambao A, et al. The Cys214–>Ser mutation in peripherin/rds causes a loss-of-function phenotype in transgenic mice. *Biochem J*. 2005;388(Pt2):605–613.
45. Cheng T, Peachey NS, Li S, et al. The effect of peripherin/rds haploinsufficiency on rod and cone photoreceptors. *J Neurosci*. 1997;17(21):8118–8128.
46. Oishi A, Fujinami K, Mawatari G, et al. Genetic and phenotypic landscape of PRPH2-associated retinal dystrophy in Japan. *Genes (Basel)*. 2021;12(11):1817.
47. Reeves MJ, Goetz KE, Guan B, et al. Genotype-phenotype associations in a large PRPH2-related retinopathy cohort. *Hum Mutat*. 2020;41(9):1528–1539.
48. Salinas RY, Baker SA, Gospe SM, et al. A single valine residue plays an essential role in peripherin/RDS targeting to photoreceptor outer segments. *PLoS One*. 2013;8(1):e54292.
49. Loewen CJR, Moritz OL, Tam BM, et al. The role of subunit assembly in peripherin-2 targeting to rod photoreceptor disk membranes and retinitis pigmentosa. *Mol Biol Cell*. 2003;14(8):3400–3413.
50. Payne AM, Downes SM, Bessant DA, et al. Founder effect, seen in the British population, of the 172 peripherin/RDS mutation-and further refinement of genetic positioning of the peripherin/RDS gene. *Am J Hum Genet*. 1998;62(1):192–195.
51. Alapati A, Goetz K, Suk J, et al. Molecular diagnostic testing by eyeGENE: analysis of patients with hereditary retinal dystrophy phenotypes involving central vision loss. *Invest Ophthalmol Vis Sci*. 2014;55(9):5510–5521.
52. Daftarian N, Mirrahimi M, Sabbaghi H, et al. PRPH2 mutation as the cause of various clinical manifestations in a family affected with inherited retinal dystrophy. *Ophthalmic Genet*. 2019;40(5):436–442.
53. Downes SM, Fitzke FW, Holder GE, et al. Clinical features of codon 172 RDS macular dystrophy: similar phenotype in 12 families. *Arch Ophthalmol*. 1999;117:1373–1383.
54. Nakazawa M, Wada Y, Tamai M. Macular dystrophy associated with monogenic Arg172Trp mutation of the peripherin/RDS gene in a Japanese family. *Retina*. 1995;15:518–523.
55. Piguet B, Heon E, Munier FL, et al. Full characterization of the maculopathy associated with an Arg-172-Trp mutation in the RDS/peripherin gene. *Ophthalmic Genet*. 1996;17:175–186.
56. Albertos-Arranz H, Sanchez-Saez X, Martinez-Gil N, et al. Phenotypic differences in a PRPH2 mutation in members of the same family assessed with OCT and OCTA. *Diagnostics*. 2021;11(5):777.
57. Trujillo MJ, Bueno J, Osorio A, et al. Three novel RDS-peripherin mutations (689delT, 857del17, G208D) in Spanish families affected with autosomal dominant retinal degenerations. Mutations in brief no. 147. *Hum Mutat*. 1998;12(1):70.
58. Birtel J, Eisenberger T, Gliem M, et al. Clinical and genetic characteristics of 251 consecutive patients with macular and cone/cone-rod dystrophy. *Sci Rep*. 2018;8(1):4824.
59. Soucy M, Kolesnikova M, Kim AH, Tsang SH. Phenotypic variability in PRPH2 as demonstrated by a family with incomplete penetrance of autosomal dominant cone-rod dystrophy. *Doc Ophthalmol*. 2023;146(3):267–272.
60. Ruiz-Pastor MJ, Sanchez-Saez X, Kutsyr O, et al. Prph2 knock-in mice recapitulate human central areolar choroidal dystrophy retinal degeneration and exhibit aberrant synaptic remodeling and microglial activation. *Cell Death Dis*. 2023;14(11):711.
61. Chen FK, Agelis L, Peh KK, et al. Visual acuity fractions derived from a Snellen chart and letter scores on the early treatment diabetic retinopathy study chart. *Asia Pac J Ophthalmol*. 2014; 3(5):277–285.
62. Heath Jeffery RC, Lo J, Thompson JA, et al. Analysis of the outer retinal bands in ABCA4 and PRPH2-associated retinopathy using OCT. *Ophthalmol Retina*. 2024;8(2):174–183. 2023 May [online ahead of print].
63. Renner AB, Fiebig BS, Weber BHF, et al. Phenotypic variability and long-term follow-up of patients with known and novel PRPH2/RDS gene mutations. *Am J Ophthalmol*. 2009;147(3):518–530.
64. Sohocki MM, Daiger SP, Bowne SJ, et al. Prevalence of mutations causing retinitis pigmentosa and other inherited retinopathies. *Hum Mutat*. 2001;17(1):42–51.
65. Koyanagi Y, Akiyama M, Nishiguchi KM, et al. Genetic characteristics of retinitis pigmentosaw in 1204 Japanese patients. *J Med Genet*. 2019;56(10)662–670.
66. Sullivan LS, Bowne SJ, Birch DG, et al. Prevalence of disease-causing mutations in families with autosomal dominant retinitis pigmentosa: a screen of known genes in 200 families. *Invest Ophthalmol Vis Sci*. 2006;47(7):3052–3064.
67. Stone EM, Andorf JL, Whitmore SS, et al. Clinically focused molecular investigation of 1000 consecutive families with

Investigative Ophthalmology & Visual Science

inherited retinal disease. *Ophthalmology*. 2017;124(9):1314–1331.
68. Khani SC, Karoukis AJ, Young JE, et al. Late-onset autosomal dominant macular dystrophy with choroidal neovascularisation and nonexudative maculopathy associated with mutation in the RDS gene. *Invest Ophthalmol Vis Sci*. 2003;44(8):3570–3577.
69. Klevering BJ, van Driel M, van Hogerwou AJM, et al. Central areolar choroidal dystrophy associated with dominantly inherited drusen. *Br J Ophthalmol*. 2002;86(1):91–96.
70. Jacobson SG, Cideciyan AV, Maguire AM, et al. Preferential rod and cone photoreceptor abnormalities in heterozygotes with point mutations in the RDS gene. *Exp Eye Res*. 1996;63(5):603–608.
71. Testa F, Marini V, Rossi S, et al. A novel mutation in the RDS gene in an Italian family with pattern dystrophy. *Br J Ophthalmol*. 2005;89(8):1066–1068.
72. Coco-Martin RM, Sanchez-Tocino HT, Desco C, et al. PRPH2-related retinal diseases: broadening the clinical spectrum and describing a new mutation. *Genes (Basel)*. 2020;11(7):773.
73. Duncan JL, Talcott KE, Ratnam K, et al. Cone structure in retinal degeneration associated with mutations in the peripherin/RDS gene. *Invest Ophthalmol Vis Sci*. 2011;52(3):1557–1566.
74. Colombo L, Maltese PE, Castori M, et al. Molecular epidemiology in 591 Italian probands with non-syndromic retinitis pigmentosa and Usher syndrome. *Invest Ophthalmol Vis Sci*. 2021;62(2):13.
75. Martin-Merida I, Aguilera-Garcia D, Fernandez-San JP, et al. Toward the mutational landscape of autosomal dominant retinitis pigmentosa: a comprehensive analysis of 258 Spanish families. *Invest Ophthalmol Vis Sci*. 2018;59(6):2345–2354.
76. Almoguera B, Li J, Fernandez-San PJ, et al. Application of whole exome sequencing in six families with an initial diagnosis of autosomal dominant retinitis pigmentosa: lessons learned. *PLoS One*. 2015:10(7):e0133624.
77. Manes G, Guillaumie T, Vos WL, et al. High prevalence of PRPH2 in autosomal dominant retinitis pigmentosa in France and characterisation of biochemical and clinical features. *Am J Ophthalmol*. 2015;159(2):302–314.
78. Carss KJ, Arno G, Erwood M, et al. Comprehensive rare variant analysis via whole-genome sequencing to determine the molecular pathology of inherited retinal disease. *Am J Hum Genet*. 2017;100(1):75–90.
79. Ekstrom U, Ponjavic V, Abrahamson M, et al. Phenotypic expression of autosomal dominant retinitis pigmentosa in a Swedish family expressing a Phe-211-Leu variant of peripherin/RDS. *Ophthalmic Genet*. 1998;19(1):27–37.
80. Zhang K, Garibaldi DC, Li Y, et al. Butterfly-shaped pattern dystrophy: a genetic, clinical, and histopathological report. *Arch Ophthalmol*. 2002;120(4):485–490.
81. Fishman GA, Stone E, Gilbert LD, et al. Clinical features of a previously undescribed codon 216 (proline to serine) mutation in the peripherin/retinal degeneration slow gene in autosomal dominant retinitis pigmentosa. *Ophthalmology*. 1994;101(8):1409–1421.
82. Ellingford JM, Barton S, Bhaskar S, et al. Molecular findings from 537 individuals with inherited retinal disease. *J Med Genet*. 2016;53(11):761–767.
83. Ahmad OR, Ayyagari R, Zacks DN. A novel missense mutation in the rds/peripherin gene associated with retinal pattern dystrophy. *Retin Cases Brief Rep*. 2010;4(1):84–85.
84. Liu X, Tao T, Zhao L, et al. Molecular diagnosis based on comprehensive genetic testing in 800 Chinese families with non-syndromic inherited retinal dystrophies. *Clin Exp Ophthalmol*. 2021;49(1):46–59.
85. de Breuk A, Acar IE, Kersten E, et al. Development of a genotype assay for age-related macular degeneration: the eye-risk consortium. *Ophthalmology*. 2021;128(11):1604–1617.
86. Huang L, Li S, Xiao X, et al. Screening for variants in 20 genes in 130 unrelated patients with cone-rod dystrophy. *Mol Med Rep*. 2013;7(6):1779–1785.
87. Kajiwara K, Hahn LB, Mukai S, et al. Mutations in the human retinal degeneration slow gene in autosomal dominant retinitis pigmentosa. *Nature*. 1991;354(6353):480–483.
88. Yang Z, Lin W, Moshfeghi DM, et al. A novel mutation in the RDS/Peripherin gene causes adult-onset foveomacular dystrophy. *Am J Ophthalmol*. 2003;135(2):213–218.
89. Sodi A, Mucciolo DP, Giorgio D, et al. Clinical and molecular findings in patients with pattern dystrophy. *Ophthalmic Genet*. 2021;42(5):577–587.
90. Weleber RG, Carr RE, Murphey WH, et al. Phenotypic variation including retinitis pigmentosa, pattern dystrophy, and fundus flavimaculatus in a single family with a deletion of codon 153 or 154 of the peripherin/RDS gene. *Arch Ophthalmol*. 1993;111(11):1531–1542.
91. van Lith-Verhoeven JJC, van den Helm B, Deutman AF, et al. A peculiar autosomal dominant macular dystrophy caused by an asparagine deletion at codon 169 in the peripherin/RDS gene. *Arch Ophthalmol*. 2003;121(10):1452–1457.
92. Kalyanasundaram TS, Black GC, O'Sullivan J, Bishop PN. A novel peripherin/RDS mutation resulting in a retinal dystrophy with phenotypic variation. *Eye(Lond)*. 2009;23(1):237–239.
93. Jin Z-B, Mandai M, Yokota T, et al. Identifying pathogenic genetic background of simplex or multiplex retinitis pigmentosa patients: a large scale mutation screening study. *Med Genet*. 2008;45(7):465–472.
94. Sullivan LS, Guilford SR, Birch DG, Daiger SP. A novel splice site mutation in the gene for peripherin/RDS causing dominant retinal degeneration. *Invest Ophthalmol Vis Sci*. 1996;37:1145.
95. Duncker T, Tsang SH, Woods RL, et al. Quantitative fundus autofluorescence and optical coherence tomography in PRPH2/RDS- and ABCA4-associated disease exhibiting phenotypic overlap. *Invest. Ophthalmol. Vis. Sci*. 2015;56(5):3159–3170.

Investigative Ophthalmology & Visual Science